AMERICAN SOCIETY FOR MICROBIOLOGY | Journal of Virology®

VACCINES AND ANTIVIRAL AGENTS

Targeting Kaposi's Sarcoma-Associated Herpesvirus ORF21 Tyrosine Kinase and Viral Lytic Reactivation by Tyrosine Kinase Inhibitors Approved for Clinical Use

Guillaume Beauclair,[a,b]* Eleonora Naimo,[a,b] Tatyana Dubich,[c] Jessica Rückert,[a,b] Sandra Koch,[a,b] Akshay Dhingra,[a,b] Dagmar Wirth,[c,d] Thomas F. Schulz[a,b,e]

[a]Institute of Virology, Hannover Medical School, Hannover, Germany
[b]German Centre for Infection Research, Hannover-Braunschweig Site, Hannover, Germany
[c]Model Systems for Infection and Immunity, Helmholtz Centre for Infection Research, Braunschweig, Germany
[d]Institute for Experimental Hematology, Hannover Medical School, Hannover, Germany
[e]Excellence Cluster 2155 RESIST, Hannover Medical School, Hannover, Germany

Guillaume Beauclair and Eleonora Naimo contributed equally to this work. Author order was determined both alphabetically and according to the duration of involvement in this project.

ABSTRACT Kaposi's sarcoma-associated herpesvirus (KSHV) is the cause of three human malignancies: Kaposi's sarcoma, primary effusion lymphoma, and the plasma cell variant of multicentric Castleman disease. Previous research has shown that several cellular tyrosine kinases play crucial roles during several steps in the virus replication cycle. Two KSHV proteins also have protein kinase function: open reading frame (ORF) 36 encodes a serine-threonine kinase, while ORF21 encodes a thymidine kinase (TK), which has recently been found to be an efficient tyrosine kinase. In this study, we explore the role of the ORF21 tyrosine kinase function in KSHV lytic replication. By generating a recombinant KSHV mutant with an enzymatically inactive ORF21 protein, we show that the tyrosine kinase function of ORF21/TK is not required for the progression of the lytic replication in tissue culture but that it is essential for the phosphorylation and activation to toxic moieties of the antiviral drugs zidovudine and brivudine. In addition, we identify several tyrosine kinase inhibitors, already in clinical use against human malignancies, which potently inhibit not only ORF21 TK kinase function but also viral lytic reactivation and the development of KSHV-infected endothelial tumors in mice. Since they target both cellular tyrosine kinases and a viral kinase, some of these compounds might find a use in the treatment of KSHV-associated malignancies.

IMPORTANCE Our findings address the role of KSHV ORF21 as a tyrosine kinase during lytic replication and the activation of prodrugs in KSHV-infected cells. We also show the potential of selected clinically approved tyrosine kinase inhibitors to inhibit KSHV TK, KSHV lytic replication, infectious virion release, and the development of an endothelial tumor. Since they target both cellular tyrosine kinases supporting productive viral replication and a viral kinase, these drugs, which are already approved for clinical use, may be suitable for repurposing for the treatment of KSHV-related tumors in AIDS patients or transplant recipients.

KEYWORDS Kaposi's sarcoma-associated herpesvirus, KSHV, ORF21, inhibitors, lytic reactivation, tumor growth, tyrosine kinase

Kaposi's Sarcoma-associated herpesvirus (KSHV), a gammaherpesvirus, causes Kaposi's sarcoma (KS), primary effusion lymphoma (PEL), and multicentric Castleman disease (MCD). KSHV-related diseases occur frequently in AIDS and other immunocom-

Citation Beauclair G, Naimo E, Dubich T, Rückert J, Koch S, Dhingra A, Wirth D, Schulz TF. 2020. Targeting Kaposi's sarcoma-associated herpesvirus ORF21 tyrosine kinase and viral lytic reactivation by tyrosine kinase inhibitors approved for clinical use. J Virol 94:e01791-19. https://doi.org/10.1128/JVI.01791-19.

Editor Richard M. Longnecker, Northwestern University

Address correspondence to Guillaume Beauclair, guillaume.beauclair@pasteur.fr, or Thomas F. Schulz, schulz.thomas@mh-hannover.de.

* Present address: Guillaume Beauclair, Unité Génomique Virale et Vaccination, Département de Virologie, CNRS UMR 3569, Institut Pasteur, Paris, France.

Received 17 October 2019
Accepted 4 December 2019
Accepted manuscript posted online 11 December 2019
Published 14 February 2020

promised patients and are particularly common in sub-Saharan Africa (1, 2). KSHV can infect endothelial cells, B cells, monocytes, epithelial cells, and keratinocytes (3). In KS tumors, mainly endothelial cells are infected, whereas infected B cells represent the neoplastic cell type in PEL and MCD. In most infected cells, KSHV persists in a latent form that is characterized by the expression of only a few viral genes. Physiological stress signals, such as hypoxia, chemicals like sodium butyrate (SB) and tetradecanoyl phorbol acetate (TPA), and ectopic expression of RTA, the product of the viral gene *ORF50*, allow the virus to switch from latency to lytic replication (4–7). During lytic replication, most viral genes are expressed and progeny virions are produced. Low levels of spontaneous viral lytic replication *in vivo* are thought to be important for persistence, dissemination, and tumorigenesis (8–14). In addition, a "relaxed" latency program (8, 15) involves the production of several viral lytic proteins with paracrine and angiogenic properties, such as viral interleukin-6 (vIL-6), viral macrophage inflammatory protein I to III (vMIP-I to -III), viral G protein-coupled receptor (vGPCR), K1, and K15 (16–32). In some cell types, the expression of a select group of lytic viral proteins such as vIL-6 and vIRF3 can occur in the absence of RTA (33–36).

Among the lytic viral proteins are two virus-encoded kinases, the viral thymidine kinase (TK, *ORF21*) and the Ser/Thr kinase (vPK, *ORF36*), and KSHV also relies on cellular kinases to regulate its replication cycle (37). Viral TKs are conserved among human alpha- and gammaherpesviruses and are encoded, respectively, by *UL23* of herpes simplex virus 1 and 2 (HSV-1/2), *ORF36* of varicella-zoster virus (VZV), *BXLF1* of Epstein-Barr virus (EBV), and *ORF21* of KSHV (Fig. 1A). They mediate the phosphorylation of pyrimidine nucleosides and prodrugs such as zidovudine (AZT), acyclovir (ACV), and brivudine (BRV) (38, 39), which subsequently undergo additional phosphorylation steps by cellular kinases to generate the active drug capable of inhibiting herpesvirus-specific DNA polymerases and viral DNA synthesis (38). Herpesviral thymidine kinases differ significantly in their ability to phosphorylate nucleosides and their analogues. Several studies have shown that KSHV TK preferentially phosphorylates pyrimidine nucleosides and is unable to efficiently phosphorylate purine analogues that are instead preferentially phosphorylated by PK/ORF36 (39, 40). A combined treatment with high doses of zidovudine and valganciclovir, which are phosphorylated and converted to toxic moieties by TK/ORF21 and PK/ORF36, respectively, gave a good clinical response against KSHV multicentric Castelman disease (41, 42). However, KSHV TK/ORF21 has an up to 60-fold higher K_m for thymidine than does HSV-1 TK and therefore phosphorylates thymidine much less efficiently (39). TK may therefore have another role in the viral life cycle and, in fact, has recently been shown to also act as a tyrosine kinase (43). KSHV TK autophosphorylates its tyrosine residues at positions 65, 85, and 120 (43, 44), which are located in the extended N-terminal domain that is characteristic for gammaherpesviruses but lacking in alphaherpesviruses (Fig. 1A). Phosphorylated TK interacts with and phosphorylates Crk family proteins and the p85 regulatory subunit of phosphatidylinositol 3-kinase (PI3-K). When KSHV TK is overexpressed by transfection, autophosphorylation of TK results in the disruption of focal adhesions and activation of Rho-ROCK-myosin II-dependent cell contraction and blebbing (43). Replacing three essential glycine residues in the ATP binding pocket (GXXGXGK) (Fig. 1A) of the kinase domain with valine leads to a dramatic decrease in TK autophosphorylation (45).

HSV-1 TK is important for reactivation from latency (46), and murine gammaherpesvirus 68 (MHV-68) mutants with a disrupted TK gene replicated normally *in vitro* but were severely attenuated *in vivo* (47, 48). Here, we show that KSHV TK and its kinase function are dispensable for lytic replication in tissue culture but required for the activation of the antiviral drugs brivudine and zidovudine in KSHV-infected cells. We also identified several clinically approved tyrosine kinase inhibitors that inhibit TK kinase function and viral lytic reactivation. Several of these inhibitors antagonized the formation of endothelial tumors in a mouse xenograft model with KSHV-infected endothelial cells. These results highlight the potential of selected Food and Drug Administration (FDA)-approved tyrosine kinase inhibitors to target KSHV TK and to inhibit KSHV lytic replication as well as KSHV tumorigenesis.

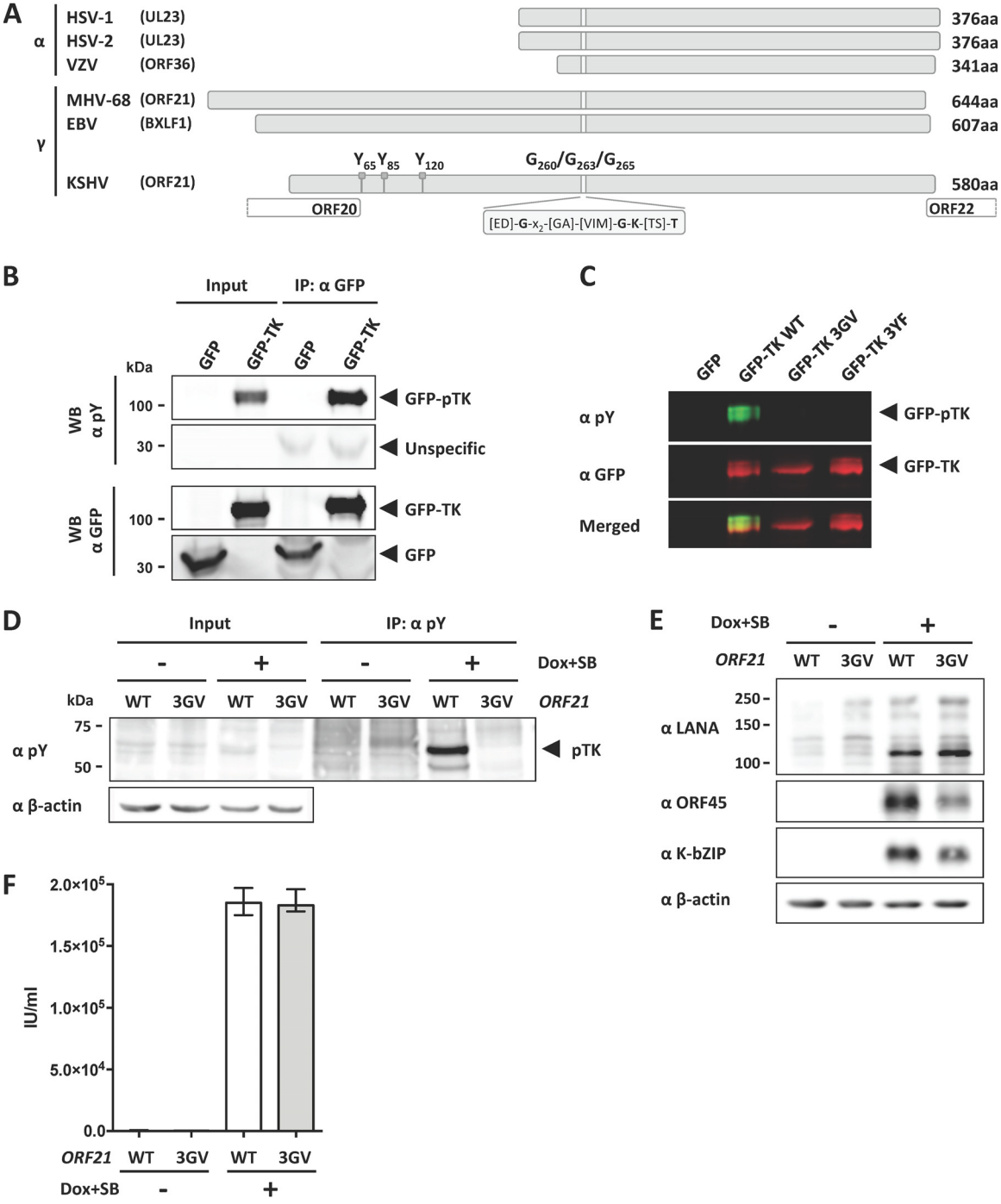

FIG 1 TK autophosphorylation is not essential for KSHV lytic replication in tissue culture. (A) Graphical representation of the TK genes from alphaherpesviruses HSV-1, HSV-2, and VZV and gammaherpesviruses EBV, KSHV, and MHV-68. Phosphorylated tyrosine residues Y_{65}, Y_{85}, and Y_{120} and glycine residues G_{260}, G_{263}, and G_{265} in the ATP binding pocket of KSHV TK are indicated. (B) GFP-TK was overexpressed by transient transfection into HEK293 cells and immunoprecipitated 48 h later using a GFP antibody. Phosphorylation of GFP-TK and total GFP-TK were estimated by immunoblotting (Western blotting [WB]) using a phosphotyrosine antibody and GFP antibody, respectively. (C) GFP or GFP-TK WT, 3GV, or 3YF (see the text) was overexpressed by transient transfection in HEK293 cells. Total lysates were analyzed 48 h after transfection by immunoblotting using antibodies to phosphorylated tyrosine residues or to GFP. (D) iSLK cells stably transfected with either KSHV BAC16 WT or the ORF21/TK ATP-binding pocket mutant KSHV BAC16 3GV (see the text) were induced with Na butyrate (SB) (1 mM) and doxycycline (1 μg/ml) to trigger lytic replication. Nonreactivated cells were used as a control. At 48 h after induction, cells were lysed, immunoprecipitated using beads coupled to an antibody against phosphorylated tyrosine residues, and analyzed by immunoblotting using antibodies against phosphorylated tyrosine (pY) and β-actin. A representative experiment is shown. Similar results were obtained with three independently generated sets of iSLK populations that had been stably transfected with KSHV-WT and KSHV-ORF21_3GV bacmids. (E) At 48 h after induction, iSLK/KSHV-WT and iSLK/KSHV-ORF21_3GV cells were lysed and analyzed by immunoblotting using antibodies against LANA, ORF45, K-bZIP, and β-actin. (F) Supernatants from reactivated and nonreactivated iSLK cells (E) were used to infect HEK293. Infected GFP-positive cells were counted 48 h after infection.

RESULTS

Mutation of the ORF21/TK ATP-binding pocket in the KSHV genome abrogates TK phosphorylation but does not interfere with the KSHV lytic cycle in tissue culture. KSHV TK has been shown to be autophosphorylated on three tyrosine residues located in the extended N-terminal domain of KSHV TK, which is typical for gammaherpesviruses (KSHV, EBV, MHV-68) but lacking in alphaherpesviruses (HSV-1, HSV-2, VZV) (Fig. 1A) (43). Replacing three essential glycine residues in the ATP binding pocket (GXXGXGK) (Fig. 1A) of the kinase domain with valine leads to a dramatic decrease in TK autophosphorylation (43, 49).

To confirm those results, we transfected an expression vector for ORF21/TK, fused to an N-terminal green fluorescent protein (GFP), into HEK293 cells and analyzed cell lysates by immunoblotting using an antibody specific for phosphorylated tyrosine residues. This revealed a phosphorylated band with a molecular weight corresponding to that of the GFP-TK fusion protein (Fig. 1B). Immunoprecipitation with an antibody to GFP showed that the phosphorylated band corresponded to the transfected GFP-TK fusion protein (Fig. 1B, top panels). To confirm that this signal is specific for TK phosphorylated on tyrosine residues, we performed a similar experiment using expression vectors for GFP alone, GFP-TK wild type (WT), and GFP-TK mutants harboring either three point mutations ($G_{260}V$, $G_{263}V$, $G_{265}V$) replacing glycine with valine residues in the ATP binding pocket (GFP-TK 3GV) (Fig. 1A) or three point mutations replacing tyrosine residues 65, 85, and 120 in the amino-terminal domain of KSHV TK with phenylalanine residues (GFP-TK 3YF) (Fig. 1A), which have been previously shown to be autophosphorylated in KSHV TK (43, 44). Neither of these mutants was recognized by the antibody to phosphorylated tyrosine residues (Fig. 1C), suggesting that the observed phosphorylation of WT TK (Fig. 1B) is due mainly to autophosphorylation and that cellular kinases are not involved in this process.

We next addressed the role of the ORF21 tyrosine kinase function during viral lytic replication. Using the KSHV BAC16 genome, we created a KSHV mutant harboring the above three point mutations ($G_{260}V$, $G_{263}V$, $G_{265}V$) in the ATP binding pocket, which inhibit the TK tyrosine kinase function (43) (Fig. 1B and C). iSLK cells were transfected with WT KSHV BAC (iSLK/BAC16 WT) and this KSHV BAC mutant (iSLK/BAC16 3GV), and stably transfected bulk populations were selected. Lytic replication was then induced in these cells by treatment with doxycycline and Na butyrate, and cells were collected 48 h after reactivation, lysed, and immunoprecipitated with an antibody recognizing phosphotyrosine (pY) residues. By immunoblotting with the same anti-phosphotyrosine antibody, we observed increased phosphorylation of a protein band of the molecular weight expected for TK (pTK, approximately 65 kDa) (43, 44) in induced iSLK/BAC16 WT cells but not in induced iSLK/BAC16 3GV cells (Fig. 1D). Similar results were obtained with three independently generated sets of iSLK populations that had been stably transfected with KSHV-WT and KSHV-ORF21_3GV bacmids. This pattern suggests that the phosphorylation of this protein during lytic reactivation is dependent on the TK tyrosine kinase function. We observed that expression of the early lytic proteins ORF45 and K-bZIP were moderately decreased (Fig. 1E), but the titer of viral progeny not affected (Fig. 1F) if the TK tyrosine kinase function was abolished. We conclude that the enzymatic function of KSHV ORF21/TK is required for efficient TK autophosphorylation in KSHV-infected cells undergoing lytic replication but is not essential for the KSHV lytic cycle in cultured epithelial cells.

ORF21/TK is required to activate brivudine and zidovudine in KSHV-infected cells. Pyrimidine nucleoside derivatives have been shown to be preferentially phosphorylated by herpesviral thymidine kinases, and purine nucleosides are preferentially activated by beta- and gammaherpesvirus protein kinases (40). Based on this evidence, we tested two pyrimidine compounds, brivudine and zidovudine, at several concentrations in iSLK cells stably infected with either KSHV-WT or the KSHV-ORF21_3GV mutant. Following induction of the lytic cycle, the production of infectious progeny virus was inhibited by both drugs in a dose-dependent manner in KSHV-WT-infected

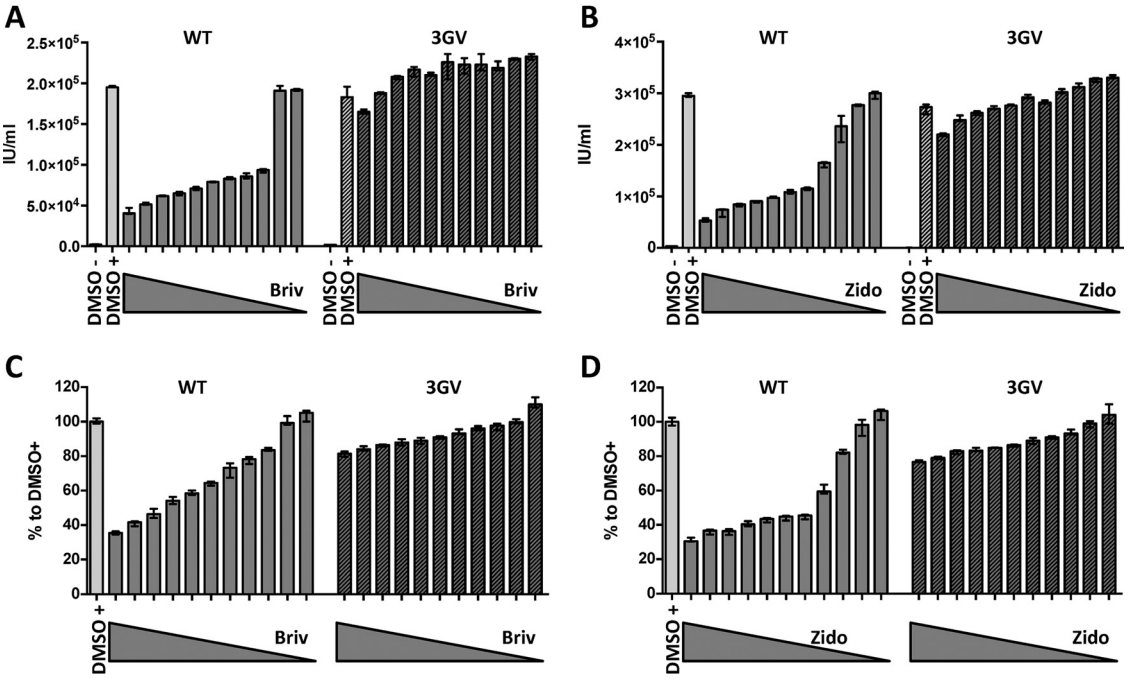

FIG 2 ORF21 is required to activate brivudine (Briv) and zidovudine (Zido). (A and B) iSLK cells stably transfected with KSHV-WT (WT) or KSHV-ORF21_3GV mutant (3GV) were induced with SB (1 mM) and doxycycline (1 μg/ml) and treated with 0.01 μM to 10 μM (1/2 dilutions) of brivudine (A) or zidovudine (B) DMSO-treated nonreactivated and reactivated cells were used as a control. Supernatants from inhibitor-treated, reactivated, and nonreactivated iSLK cells were used to infect HEK293. Infected GFP-positive cells were counted 48 h after infection. (C and D) MTT assay of iSLK cells was performed 48 h after treatment with inhibitors and reactivation.

cells but not in KSHV-ORF21_3GV-infected cells, suggesting that the KSHV-ORF21_3GV mutant is resistant to both compounds (Fig. 2A and B). Cell viability, evaluated using an MTT [3-(4,5-dimethyl-2-thiazolyl)-2,5-diphenyl-2H-tetrazolium bromide] assay, strongly decreased with increasing concentrations of brivudine and zidovudine for KSHV-WT-infected iSLK cells but only moderately for KSHV-ORF21_3GV-infected iSLK cells (Fig. 2C and D), suggesting that KSHV TK promotes the conversion of brivudine and zidvudine into cytotoxic moieties in KSHV-infected cells.

Tyrosine kinase inhibitors approved for clinical use inhibit KSHV TK (*ORF21*) autophosphorylation. We next explored if tyrosine kinase inhibitors that are approved by the FDA for clinical use could inhibit the ORF21/TK tyrosine kinase activity.

Using the assay described in the legend to Fig. 1B, we investigated whether any of 27 FDA-approved kinase inhibitors (Table 1) are able to inhibit KSHV ORF21/TK autophosphorylation. Twenty-four hours after transfection, HEK293 cells expressing GFP-TK were treated with 1 μM each inhibitor (Fig. 3). We observed that the level of autophosphorylated TK was markedly (at least 80%) decreased by bosutinib, dasatinib, and ponatinib and to a lesser extent by gefitinib and nilotinib (Fig. 3). These results suggest that these drugs are able to inhibit ORF21/TK kinase activity.

We confirmed these results in an *ex cellulo* assay, in which we performed a kinase assay on immunoprecipitated GFP-TK. Forty-eight hours after transfection of HEK293 cells with GFP-TK as described above, GFP-TK was immunoprecipitated with an antibody to GFP and immune complexes were incubated, in the presence or absence of ATP, with bosutinib, dasatinib, ponatinib, gefitinib, or nilotinib or with dimethyl sulfoxide (DMSO) as a solvent control. Autophosphorylation levels of TK were estimated by immunoblotting using an anti-phosphotyrosine antibody. The results indicate that the tested compounds inhibit autophosphorylation of immunoprecipitated TK *in vitro* in the absence of other cellular proteins (Fig. 4A). To exclude the possibility that an associated cellular kinase might have coimmunoprecipitated with ORF21/TK and caused its phosphorylation, we analyzed the ability of the "kinase-dead" GFP-TK 3GV

TABLE 1 FDA-approved kinase inhibitors used in this study[a]

Agent (designation)	Drug name	Sponsor	Date of FDA approval	Kinase inhibitor[b]	Primary target(s)
Afatinib (Gilotrif)	Tovok	Boehringer Ingelheim	July 2013	Y	EGFR, ErbB2/4
Axitinib (AG013736)	Inlyta	Pfizer	January 2012	Y	VEGFRs, c-Kit, PDGFRβ
Bosutinib (SKI-606)	Bosulif	Wyeth	September 2012	Y	BCR-Abl, Src, Lyn, Hck
Cabozantinib (XL184)	Cometriq	Exelixis	November 2012	Y	VEGFRs, c-Met, Ret, Kit, TrkB, Flt3, Tie2, Axl
Ceritinib (LDK378)	Zykadia	Novartis	April 2014	Y	ALK, IGF-1R, InsR, ROS1
Crizotinib (PF-02341066)	Xalkori	Pfizer	August 2011	Y	ALK, c-Met (HGFR), ROS1, MST1R
Dabrafenib (6964)	Tafinlar	GlaxoSmithKline	May 2013	S/T	B-Raf
Dasatinib (BM-354825)	Sprycel	Bristol-Myers Squibb	June 2006	Y	BCR-Abl, Src, Lck, Lyn, Yes, Fyn, c-Kit, EphA2, PDGFRβ
Erlotinib (OSI-744)	Tarceva	(OSI)pharmaceuticals	November 2004	Y	EGFRs
Gefitinib (ZD1839)	Iressa	AstraZeneca	May 2003	Y	EGFRs, PDGFR
Ibrutinib (PCI-32765)	Imbruvica	Pharmacyclics	November 2013	Y	BTK
Imatinib (STI571)	Gleevec	Novartis	May 2001	Y	BCR-Abl, c-Kit, PDGFR
Lapatinib (GW2016)	Tykerb	GlaxoSmithKline	March 2007	Y	EGFR, ErbB2
Lenvatinib (E7080)	Lenvima	Eisai	February 2015	Y	VEGFRs, PDGFRs, FGFRs, Kit, RET
Nilotinib (AMN107)	Tasigna	Novartis	October 2007	Y	BCR-Abl, PDGFR, Kit, DDR1
Nintedanib (BIBF1120)	Ofev	Boehringer Ingelheim	October 2014	Y	VEGFRs, FGFRs, PDGFRs, Lck
Palbocicnib (PD-0332991)	Ibrance	Pfizer	February 2015	S/T	CDK4, CDK6
Pazopanib (GW-786034)	Votrient	GlaxoSmithKline	October 2009	Y	VEGFRs, PDGFRs, FGDRs, c-Kit, Lck, Fms, Itk
Ponatinib (AP24534)	Iclusig	Ariad	December 2012	Y	BCR-Abl, PDGFRs, VEGFRs, FGFRs, Src, EphR, Kit, RET, Tie2, Flt3
Regorafenib (BAY 73-4506)	Stivarga	Bayer	September 2012	Y/S/T	VEGFRs, PDGFRs, Kit, RET, Raf-1, Tie2, EphA2
Ruxolitinib (INC424)	Jakafi	Incyte	November 2011	Y	JAK1/2
Sorafenib (BAY 43-9006)	Nexavar	Bayer	December 2005	Y/S/T	VEGFRs, PDGFRs, B-Raf, Kit, Flt3, RET, CDK8
Sunitinib (SU11248)	Sutent	Pfizer	January 2006	Y	VEGFRs, PDGFRs, c-Kit, RET, Flt3
Tofacitinib (CP-690550)	Xeljanz	Pfizer	November 2012	Y	JAK3
Trametinib (6495)	Mekinist	GlaxoSmithKline	May 2013	S/T	MEK1/2
Vandetanib (ZD6474)	Caprelsa	AstraZeneca	April 2011	Y	VEGFRs, EGFRs, RET, Tie2, Brk, EphR
Vemurafenib (PLX4043)	Zelboraf	Roche	August 2011	S/T	Raf

[a]FDA-approved small-molecule kinase inhibitors. More details may be found in reference 97.
[b]Inhibiting phosphorylation of tyrosine (Y), serine (S) or threonine (T) residues.

mutant to autophosphorylate under the same conditions (Fig. 4A). We observed no significant phosphorylation with this mutant, indicating that the observed phosphorylation is due mainly to autophosphorylation of TK. A similar experiment was performed using increasing concentrations of inhibitors (Fig. 4B). We observed that in contrast to imatinib, which did not show significant inhibition, dasatinib strongly inhibits the autophosphorylation of TK, even at 0.3 μM. Similar results were observed for bosutinib and ponatinib. In this kinase assay performed with immunoprecipitated TK, ibrutinib, which did not inhibit TK autophosphorylation in transfected cells at 1 μM (Fig. 3), was able to inhibit TK autophosphorylation by more than 50% at concentrations of 2.5 μM and higher (Fig. 4B).

Kinase inhibitors inhibit TK autophosphorylation in KSHV-infected cells. We further analyzed the impact of selected kinase inhibitors on TK autophosphorylation in KSHV-infected cells. Following induction of lytic replication in iSLK/KSHV-WT and treatment for 48 h with 5 or 10 μM dasatinib (Fig. 5A), bosutinib (Fig. 5B), or ponatinib (Fig. 5C), we immunoprecipitated phosphorylated proteins as shown in Fig. 1D. The phosphorylated band corresponding to TK was abolished by all three inhibitors at both concentrations used (Fig. 5A to C). All three compounds also strongly inhibited the production of infectious virus (Fig. 5D).

Since a KSHV mutant with an enzymatically inactive TK was not strongly compromised in reactivation from latency and production of infectious viral progeny (Fig. 1D to F), it is unlikely that the ability of these three tyrosine kinase inhibitors to inhibit virus production was linked to their inhibition of TK autophosphorylation (Fig. 3 to 5). To confirm this conclusion, we compared the concentrations of dasatinib required to inhibit KSHV-WT and the KSHV-3GV mutant carrying an enzymatically inactive TK gene (Fig. 1D). As shown in Fig. 5E, the KSHV-3GV mutant was still inhibited by dasatinib in

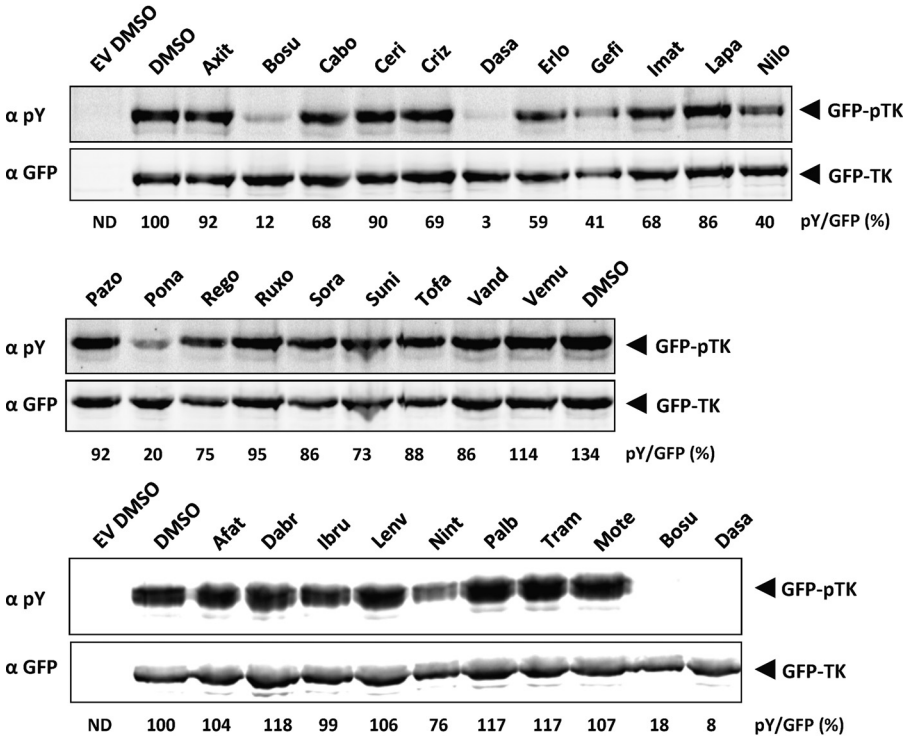

FIG 3 Autophosphorylation of TK in transfected cells can be inhibited by FDA-approved kinase inhibitors. Plasmids coding for GFP-TK or its empty vector (EV) were transfected in HEK293 cells. At 24 h after transfection, cells were treated for an additional 24 h with 1 μM FDA-approved inhibitors. Total lysates were analyzed by immunoblotting using antibodies to phosphorylated tyrosine residues or to GFP. The total GFP signal was used to normalize the ratio of phosphorylated forms of TK to total TK. See Table 1 for the complete names of the inhibitors.

a dose-dependent manner, in contrast to its resistance to brivudine (Fig. 2). This suggests that the ability of dasatinib and other tyrosine kinase inhibitors to inhibit KSHV reactivation is likely due to their inhibition of cellular tyrosine kinases.

Inhibition of KSHV lytic reactivation by FDA-approved kinase inhibitors in different cell types. To further explore the inhibition of KSHV reactivation by FDA-approved kinase inhibitors, we tested their effect on KSHV lytic replication in B cells (BJAB-rKSHV.219), endothelial cells (HuARLT-rKSHV.219), and another epithelial cell line (Vero-rKSHV.219), in which the lytic cycle was activated by different means. In BJAB-rKSHV.219 cells, the lytic cycle was induced using an antibody to IgM (50), and in HuARLT-rKSHV.219 and Vero-rKSHV.219 cells, it was induced with a baculovirus expressing RTA in combination with Na butyrate. The titer of infectious KSHV released from BJAB-rKSHV.219 cells was measured by infecting HEK293 cells as described above, and the strength of the GFP signal in infected HEK293 cells was quantified using a fluorimeter 48 h after infection (Fig. 6A). For the HuARLT-rKSHV.219 (Fig. 6B) and Vero-rKSHV.219 (Fig. 6C) cells, the number of red fluorescent protein (RFP)-expressing cells, i.e., cells undergoing lytic reactivation, was determined by microscopy 48 h after treatment. Inhibitor-treated cells were stained with MTT (BJAB-rKSHV.219) or DAPI (4′,6-diamidino-2-phenylindole) (HuARLT-rKSHV.219, Vero-rKSHV.219) to assess cell viability.

Dasatinib, ponatinib, ibrutinib, cabozantinib, lenvatinib, and trametinib inhibited virus release from induced BJAB-rKSHV.219 cells at nontoxic concentrations (Fig. 6A). Crizotinib, pazopanib, and regorafenib inhibited virus release to a lesser extent in this assay. Dasatinib, ponatinib, ibrutinib, and trametinib also lowered the expression of the KSHV early protein K-bZIP in BJAB-rKSHV.219 cells (Fig. 7A). Bosutinib, an inhibitor of ORF21/TK activity (Figs. 3 and 4), inhibited virus release in KSHV-infected endothelial

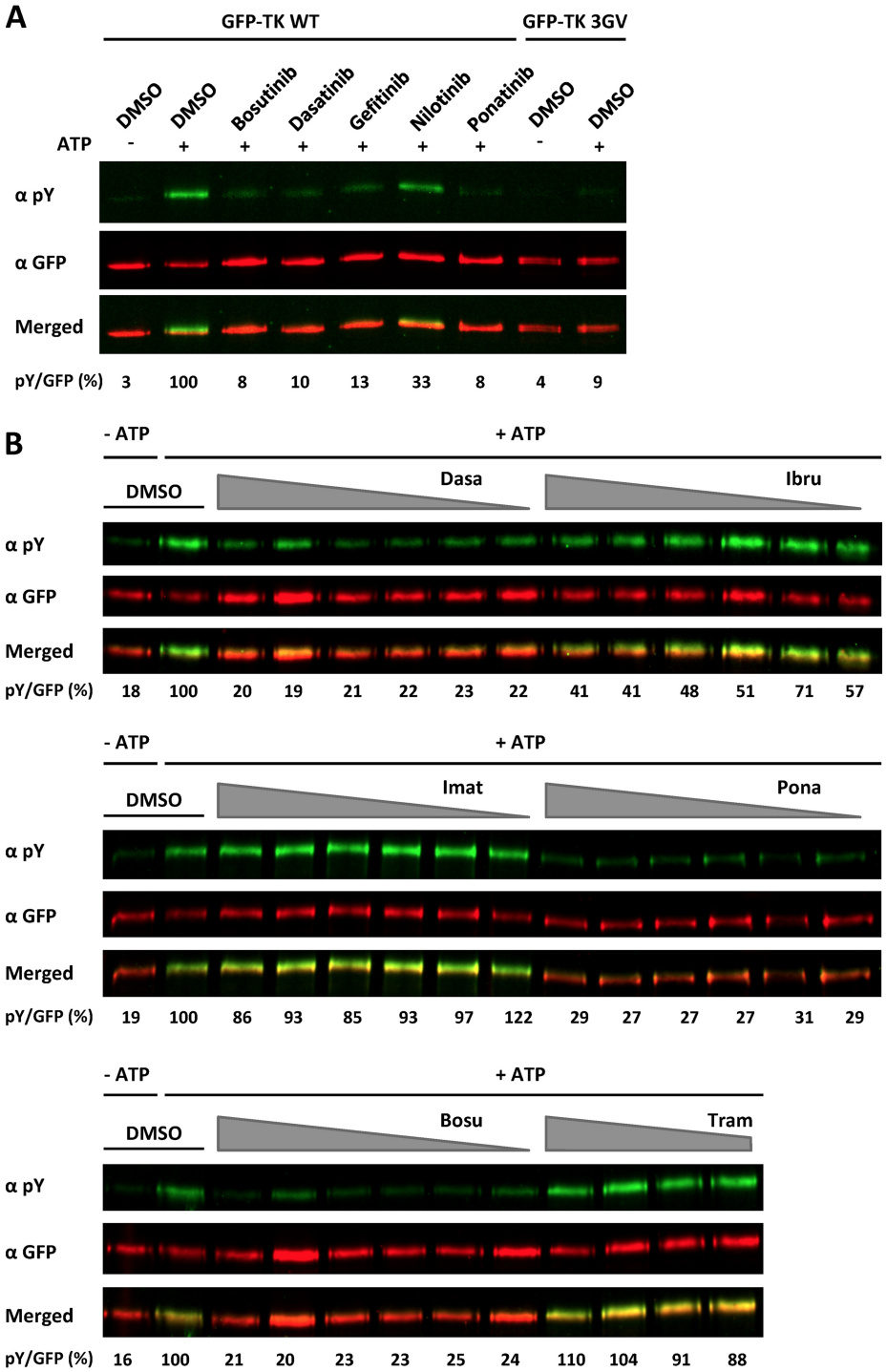

FIG 4 FDA-approved kinase inhibitors inhibit autophosphorylation of immunoprecipitated TK. (A) GFP-TK was overexpressed in HEK293 cells and immunoprecipitated 48 h later using a GFP antibody prior to an *in vitro* kinase assay in the presence or absence of ATP and 20 μM FDA-approved inhibitors. The level of phosphorylated and total TK was estimated by immunoblotting, using antibodies to phosphorylated tyrosine residues and GFP, respectively, and quantification on a Li-Cor instrument. The ratio of phosphorylated GFP-TK to total GFP in the presence of inhibitor in comparison to the DMSO control was calculated and is given below the corresponding immunoblots. (B) Similar experiment as that described for panel A with 10, 5, 2.5, 1.25, 0.625, and 0.313 μM bosutinib (Bosu), dasatinib (Dasa), ibrutinib (Ibru), imatinib (Imat), and ponatinib (Pona) and 10, 5, 2.5, and 1.25 μM trametinib (Tram).

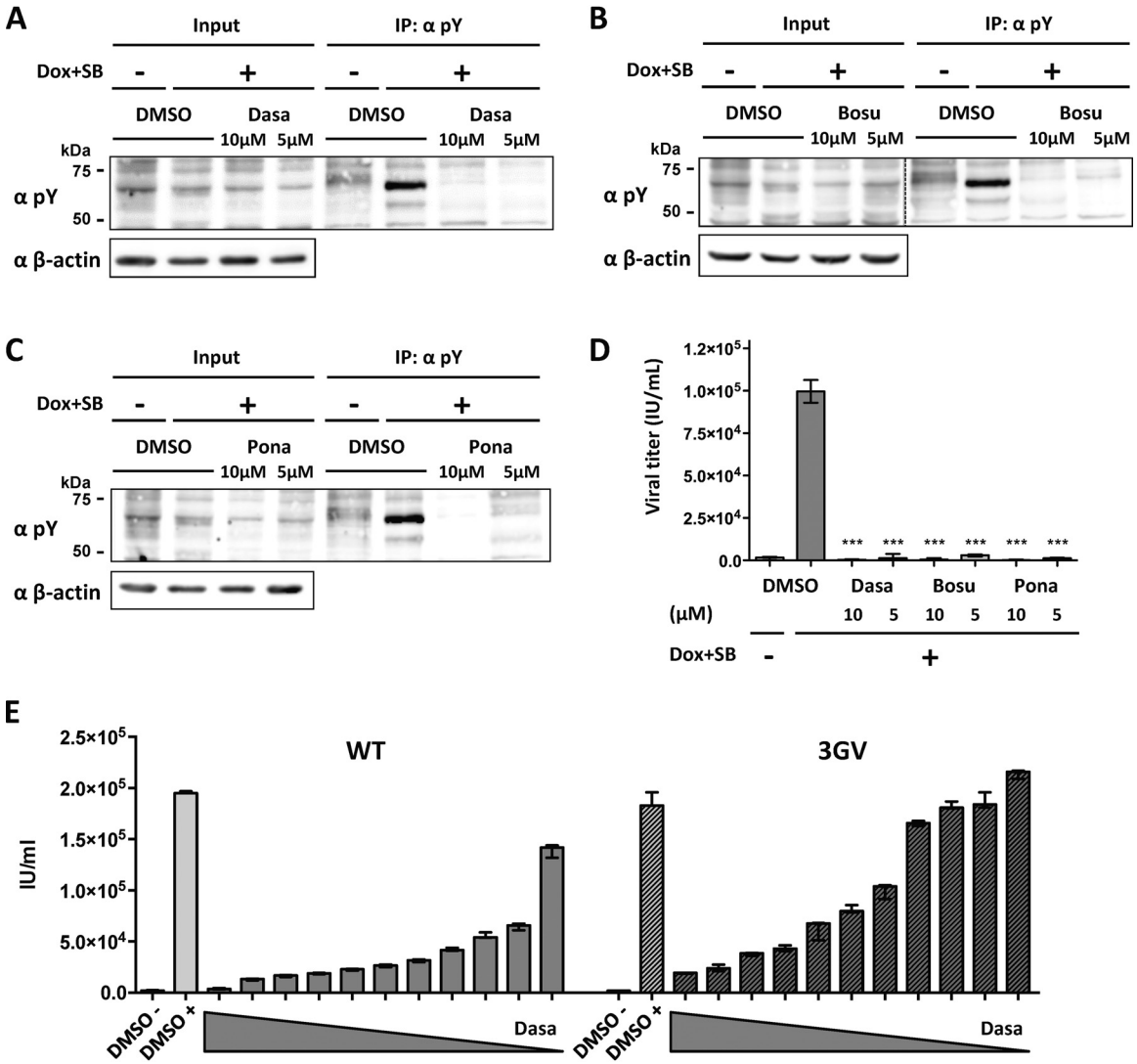

FIG 5 Inhibition of TK autophosphorylation and virus production by kinase inhibitors in KSHV-infected cells. (A to D) iSLK cells stably transfected with KSHV BAC16 WT were induced with SB (1 mM) and doxycycline (1 μg/ml) and treated with 5 or 10 μM dasatinib (A), bosutinib (B), or ponatinib (C). Nonreactivated cells were used as a control. At 48 h after induction, cells were lysed, immunoprecipitated using beads coupled to an antibody against phosphorylated tyrosine residues, and analyzed by immunoblotting using antibodies against phosphorylated tyrosine residues (pY) and β-actin. (D) Supernatants from inhibitor-treated, reactivated and nonreactivated iSLK cells were used to infect HEK293. Infected GFP-positive cells were counted 48 h after infection. An unpaired *t* test was performed. ***, $P < 0.001$. (E) Dasatinib treatment of cells infected with KSHV-WT or the KSHV-3GV mutant. iSLK cells stably transfected with KSHV-WT (WT) or the KSHV-ORF21_3GV mutant (3GV) were induced with SB (1 mM) and doxycycline (1 μg/ml) and treated with 0.01 μM to 10 μM (1/2 dilutions) of dasatinib. DMSO-treated, nonreactivated and reactivated cells were used as a control. Supernatants from inhibitor-treated, reactivated and nonreactivated iSLK cells were used to infect HEK293 cells. Infected GFP-positive cells were counted 48 h after infection.

(HuARLT-rKSHV.219) and epithelial (Vero-rKSHV.219) cells (Fig. 6B and C) but increased K-bZIP expression (Fig. 7A) and virus production (Fig. 6A) in BJAB-rKSHV.219 cells. Trametinib, a serine/threonine kinase inhibitor, inhibits the lytic replication cycle without inhibiting TK autophosphorylation (Fig. 3, 6A, and 7A).

The fact that dasatinib, ponatinib, ibrutinib, and trametinib decreased the expression of the early KSHV protein K-bZIP in KSHV-infected cells (Fig. 7A) indicates that they act at the level of virus reactivation. To assess if they might also inhibit viral entry, we tested several FDA-approved kinase inhibitors in a KSHV entry assay. We infected HEK293 cells with a stock of KSHV.219, applied the inhibitors at two concentrations (1 and 10 μM) at the time of infection, and scored the number of GFP-positive HEK293 cells after 48 h. We observed moderate inhibition at 10 μM for bosutinib, ponatinib, and dasatinib, while only ponatinib inhibited KSHV entry at 1 μM (Fig. 7B). Since dasatinib

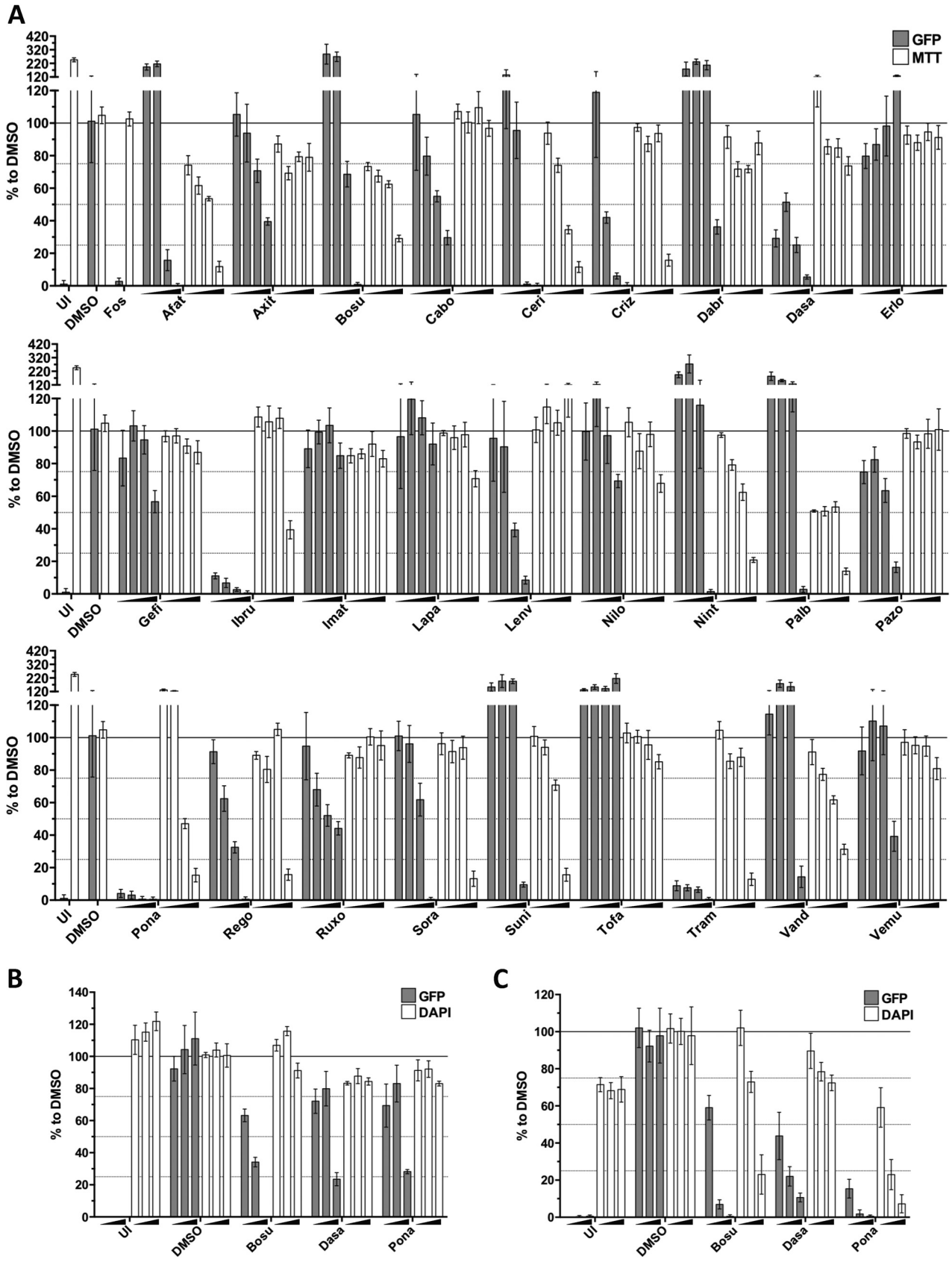

FIG 6 Inhibition of KSHV progeny production by FDA-approved tyrosine kinase inhibitors. BJAB-rKSHV.219 (A), HuARLT-rKSHV.219 (B), and Vero-rKSHV.219 (C) cells were used to estimate the inhibitory effect of several FDA-approved kinase inhibitors on KSHV lytic replication. Supernatants from

(Continued on next page)

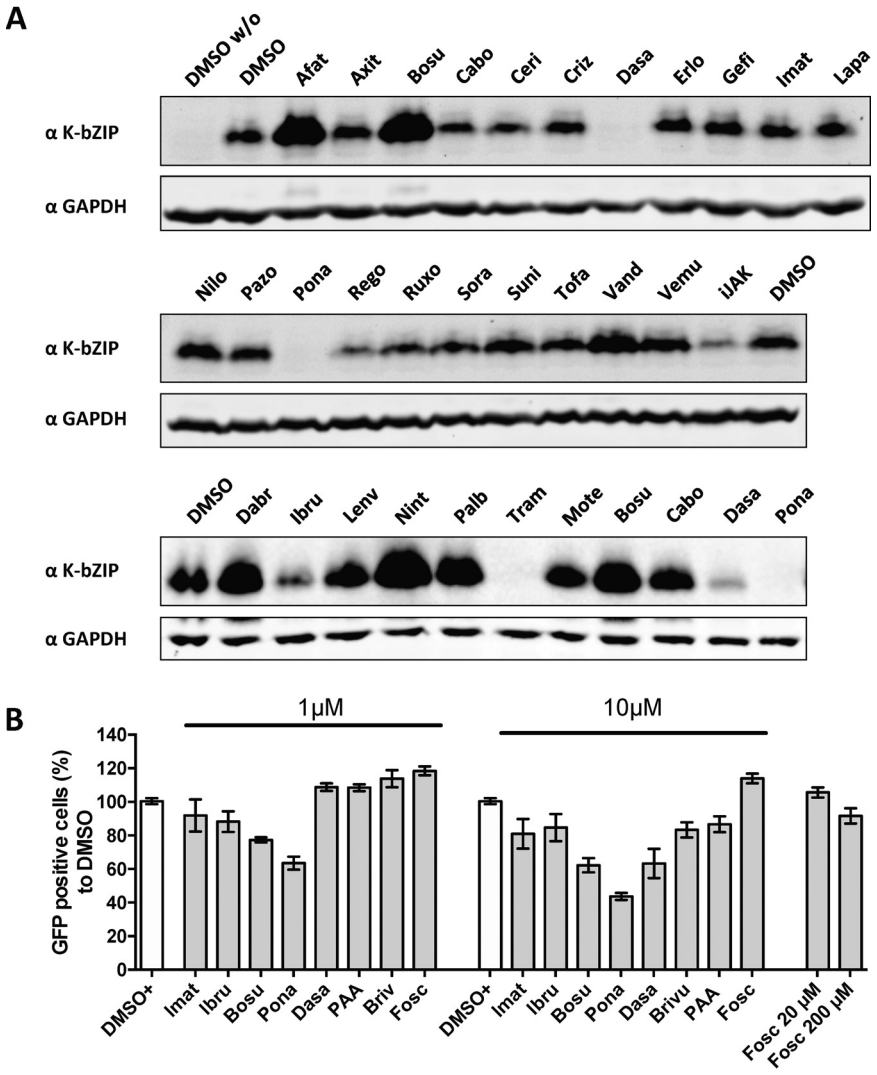

FIG 7 Inhibition of KSHV early protein expression by FDA-approved tyrosine kinase inhibitors. (A) BJAB-rKSHV.219 cells were treated with 1 μM inhibitors and triggered for reactivation (anti-IgM) for 48 h prior to lysis and analysis by immunoblotting with antibodies to the early KSHV proteins K-bZIP and ORF45. See Table 1 for the complete names of the inhibitors. (B) HEK293 cells were infected with rKSHV.219 (MOI, 1) and treated with 1 μM or 10 μM inhibitors at the time of infection. Infected GFP-positive cells were counted 48 h after infection.

potently inhibits K-bZIP expression already at 1 μM (Fig. 7A) and inhibits virus production at concentrations well below 1 μM (Fig. 5E), we conclude that it inhibits KSHV mainly at the stage of lytic cycle induction.

Inhibition of KSHV-induced tumor formation by FDA-approved kinase inhibitors. To assess the effect of selected inhibitors on KSHV-induced tumor formation *in vivo*, we implanted HuARLT-rKSHV spheroids (51) subcutaneously into mice and treated these with dasatinib, ibrutinib, imatinib, or ponatinib via oral gavage. Four weeks later, the diameter of the tumors was measured. We observed that dasatinib and imatinib

FIG 6 Legend (Continued)
reactivated, inhibitor-treated cells were used to infect HEK293 cells, and the GFP signal in HEK293 cells was measured with a luminometer 48 h after infection. Data obtained from treatments with 0.3 μM, 1 μM, 3 μM, and 10 μM (A) and 0.1 μM, 1 μM, and 10 μM (B and C) concentrations of the mentioned compounds were normalized to that with DMSO. Background signal was estimated by the signal obtained from uninduced cells (UI). Foscarnet (Fos) was used as a positive control at 200 μM. Cell toxicity was assessed by an MTT assay (BJAB-rKSHV.219) or DAPI staining (HuARLT-rKSHV.219, Vero-rKSHV.219). See Table 1 for the complete names of the inhibitors. Bars and error bars represent means ± SD across quadruplicate (A), triplicate (B) results and two datasets, each performed in triplicate (C).

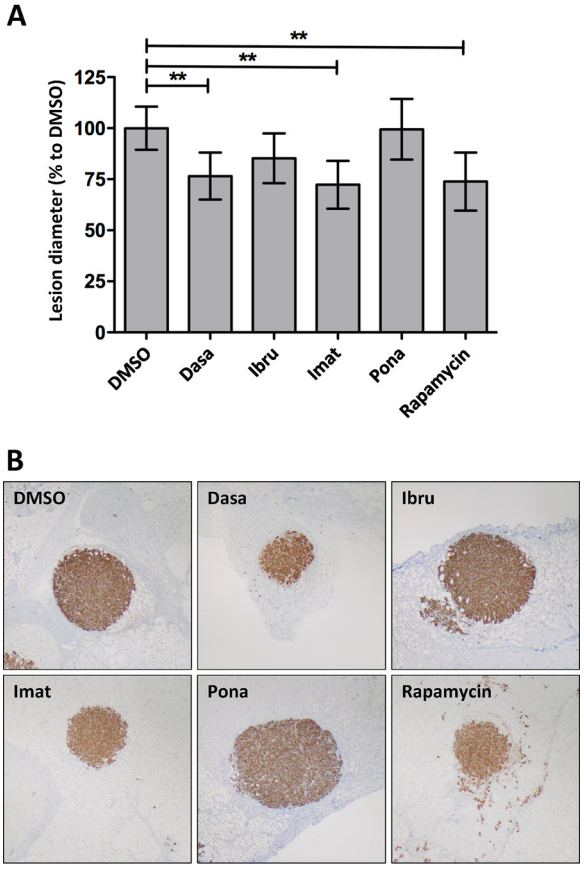

FIG 8 Inhibition of KSHV-induced tumorigenesis by FDA-approved kinase inhibitors. (A) After implantation of HuARLT-rKSHV spheroids in mice, animals were treated via oral gavage 6 times a week with dasatinib (Dasa), ibrutinib (Ibru), imatinib (Imat), and ponatinib (Pona) at concentrations of 30 mg/kg, 50 mg/kg, 100 mg/kg, and 30 mg/kg, respectively. Rapamycin (2 mg/kg) was injected 3 times a week. Four weeks later, the lesion diameter was estimated. One-way ANOVA, followed by Dunnetts' multiple comparison, was performed. *, $P < 0.05$. (B) Representative pictures of lesions.

were as potent as rapamycin in this mouse model and reduced the tumor diameter by around 25% (Fig. 8).

DISCUSSION

In this study, we explored the role of the recently described (43) tyrosine kinase function of the KSHV ORF21/thymidine kinase in KSHV lytic replication and show that it can be inhibited by several tyrosine kinase inhibitors that are already approved for clinical use. Replacing WT ORF21 with a "kinase-dead" triple mutant ORF21 gene in a recombinant KSHV genome (Fig. 1D to F) did not strongly interfere with the lytic replication in cultured epithelial cells (iSLK cells). This result is in line with the previously reported observation that MHV-68 ORF21/TK is dispensable for productive MHV-68 replication in cell culture but required for viral productive replication in the lungs of infected mice (47, 48). Therefore, it is conceivable that the tyrosine kinase function of KSHV ORF21/TK may play a role in KSHV replication in infected patients. In cells transfected with an ORF21/TK expression vector, its tyrosine kinase function contributes to morphological changes in ORF21/TK-expressing cells (43). In our experiments with the KSHV-ORF21_3GV virus, whose tyrosine kinase function is deficient, we did not observe any changes in cell morphology between KSHV-WT-infected cells and KSHV-ORF21_3GV-infected cells. This may be due to the lower level of expression of ORF21/TK in KSHV-infected cells than in ORF21/TK-transfected cells or the fact that there were relatively few cells undergoing KSHV lytic reactivation in our induced cultures.

TK preferentially phosphorylates pyrimidine nucleosides, and it is unable to effi-

ciently phosphorylate purine analogues (39, 40). When MHV-68 and herpesvirus saimiri (HVS) were passaged repeatedly in the presence of brivudine, resistance mapped to mutations in their ORF21/TK genes (40). In keeping with this observation, we show here that a "kinase-dead" KSHV mutant, KSHV-ORF21_3GV, is resistant to brivudine (Fig. 2A and C), underlining the importance of KSHV ORF21/TK for the activation of brivudine in infected cells to become an effective antiviral drug. We found the same for zidovudine (Fig. 2B and D). This observation is in line with the successful use of high-dose zidovudine in combination with valganciclovir to treat patients with active multicentric Castelman disease (41, 42).

In view of the tyrosine kinase function of KSHV ORF21/TK and the essential role of MHV-68 TK for virus replication *in vivo* (47, 48), we next explored if tyrosine kinase inhibitors that are already available for clinical use could inhibit the enzymatic activity of KSHV ORF21/TK. We screened FDA-approved inhibitors of cellular tyrosine kinases for compounds that are able to inhibit the enzymatic activity of ORF21/TK and/or KSHV lytic replication. We identified bosutinib, dasatinib, and ponatinib as potent inhibitors of ORF21/TK autophosphorylation in ORF21/TK-transfected cells (Fig. 3), in an *in vitro* kinase assay using immunoprecipitated ORF21/TK (Fig. 4) and in KSHV-infected iSLK/BAC16 cells (Fig. 5). In ORF21/TK-transfected cells, or against immunoprecipitated ORF21/TK, gefitinib, nilotinib, and nintedanib showed moderate inhibition of ORF21/TK autophosphorylation (Fig. 3 and 4). While the two most potent inhibitors of ORF21/TK autophosphorylation, dasatinib and ponatinib, all strongly inhibited KSHV lytic replication in B, endothelial, and epithelial cells and expression of the KSHV early protein K-bZIP, the three less potent compounds, gefitinib, nilotinib and nintedanib, did not (Fig. 6 and 7). Dasatinib was not toxic in any of the three cell lines tested, while bosutinib and ponatinib showed some toxicity in KSHV-infected BJAB and Vero cells (Fig. 6).

Four other cellular tyrosine kinase inhibitors, ibrutinib, lenvatinib, cabozantinib, and pazopanib, also inhibited KSHV lytic replication at nontoxic concentrations in at least one of the three tested cell lines without inhibiting ORF21/TK enzymatic activity (Fig. 3, 4, 6 and 7). As expected, trametinib, a serine/threonine inhibitor (Table 1), did not inhibit ORF21/TK autophosphorylation (Fig. 3 and 4) but potently inhibited KSHV lytic reactivation (Fig. 6 and 7).

The observation that the "kinase-dead" KSHV-ORF21_3GV mutant was not compromised in its ability to undergo lytic reactivation (Fig. 1D to F) suggested that the antiviral properties of dasatinib, ponatinib, and bosutinib in tissue culture (Fig. 5 to 7) are not dependent on their ability to inhibit ORF21/TK autophosphorylation (Fig. 3 and 4). We confirmed this conclusion by showing that the KSHV-ORF21_3GV mutant is still susceptible to inhibition by dasatinib (Fig. 5E). The ability of these tyrosine kinase inhibitors to target cellular kinases is therefore the most likely explanation for their antiviral properties in tissue culture. However, taken together, our results suggest that in patients with active KSHV replication, as observed in cases of florid KS (52, 53) and MCD (54–56), dasatinib or other tyrosine kinase inhibitors with activity against ORF21/TK might have a dual effect, targeting both cellular tyrosine kinases and the kinase function of ORF21/TK, which is, at least in the case of the animal model provided by MHV-68, required for *in vivo* lytic replication (47, 48).

There is already clinical evidence that tyrosine kinase inhibitors may play a role in the treatment of KSHV-associated disease. Imatinib mesylate has been used in phase I and II clinical trials in AIDS-related cutaneous KS (Clinical Trial no. NCT00090987) and achieved a partial regression of cutaneous KS lesions in some patients (57, 58). Inhibition of c-kit and/or platelet-derived growth factor (PDGF) receptors by imatinib may have contributed to this observation (59, 60). However, imatinib does not inhibit the tyrosine kinase function of KSHV ORF21/TK (Fig. 3 and 4) and was less efficient in inhibiting the KSHV lytic replication than dasatinib, bosutinib, ponatinib, and ibrutinib (Fig. 6 and 7). It is therefore unlikely to target KSHV directly *in vivo*.

Dasatinib is more potent than imatinib in inhibiting c-kit (dissociation constants [K_d] of 0.85 nM and 13 nM, respectively) and PDGFRβ (K_d of 0.63 nM and 14 nM, respectively) (61, 62) and also targets Abl, EphA2, and Src family kinases (SFKs). By targeting

SFKs and PDGFRβ, dasatinib inhibits several pathways which are activated during the KSHV life cycle (63–65). Dasatinib also inhibits EphA2, a receptor tyrosine kinase (RTK) involved in KSHV entry and signaling (66–69). Our results suggest that it is also a potent inhibitor of ORF21/TK phosphorylation and KSHV lytic reactivation in three different cell types without apparent cell toxicity. Dasatinib could therefore be a promising candidate to be evaluated as a treatment of KS or MCD. Dasatinib has already been used in a phase I clinical trial to treat patients with lymphoma, including EBV-associated lymphoma (Clinical Trial no. NCT00608361).

Like dasatinib, ponatinib is a multitarget kinase inhibitor. Even though ponatinib strongly inhibits KSHV replication, it was toxic in our assays and its use in patients with chronic myelogenous leukemia (CML) is known to be associated with occasional severe side effects (70).

Bosutinib, the third potent inhibitor of ORF21/TK, inhibited lytic replication in KSHV-infected endothelial and epithelial cells but increased virus production in anti-IgM-stimulated KSHV-infected BJAB cells, raising the possibility that it might promote the reactivation of KSHV from latently infected B cells *in vivo*. We hypothesize that bosutinib may also target cellular kinases that downregulate lytic replication in B cells. As reported previously, cellular Tousled-like kinases (TLKs) repressed KSHV reactivation from latency (71).

Ibrutinib mainly targets Bruton's tyrosine kinase (BTK), a nonreceptor tyrosine kinase involved in the BCR signaling pathway, which is known to activate KSHV from latency in B cells (50). In our experimental systems, ibrutinib potently inhibited KSHV reactivation not only from B cells but also from endothelial and epithelial cells (Fig. 6 and 7). It showed moderate activity against the ORF21/TK tyrosine kinase function (Fig. 4). Ibrutinib has already been used in a phase III clinical trial (Clinical Trial no. NCT01109069) in patients with chronic lymphocytic leukemia and B-cell lymphoma, including EBV-associated lymphoma (72), and may therefore be another candidate drug against KS that would merit evaluation in clinical trials.

Sorafenib, a dual tyrosine and serine/threonine protein kinase inhibitor, mainly targets VEGFR, PDGFR, and Raf kinases and has been used in a phase I/II clinical trial to treat KSHV-associated cancer (Clinical Trial no. NCT00287495). It also inhibits the human cytomegalovirus (HCMV) replication cycle (73). Sorafenib showed a moderate inhibition of KSHV lytic replication in BJAB-rKSHV.219 cells (μM range) but was toxic at higher concentrations (Fig. 6).

We also evaluated the ability of dasatinib, ibrutinib, and ponatinib to inhibit the growth of tumors developing after implantation of HuARLT-rKSHV spheroids into mice. We used rapamycin and imatinib as a reference, as these compounds have been shown to ameliorate posttransplant and AIDS KS in clinical trials (57, 58, 74, 75). We observed that dasatinib reduced tumor size in implanted mice to approximately the same degree as imatinib and rapamycin (Fig. 8).

Unlike ganciclovir, which targets the viral DNA polymerase and thereby a late stage of viral replication and which has previously been shown to reduce the risk for the subsequent emergence of KS in AIDS patients treated for CMV (76), the tyrosine kinase inhibitors identified in this study inhibit the early phase of lytic replication. This would have the advantage of decreasing the expression of early KSHV proteins with paracrine and angiogenic properties that are thought to contribute to KSHV pathogenesis, such as vIL-6, vMIP-I to -III, vGPCR, K1, and K15 (16, 17, 25, 77–83).

In conclusion, we show that several tyrosine kinase inhibitors, including dasatinib, ibrutinib, and ponatinib, are inhibitors of both ORF21/TK tyrosine kinase activity and KSHV lytic replication. While their antiviral effect in tissue culture is due mostly to their ability to inhibit cellular tyrosine kinases, these compounds may have the advantage of targeting cellular tyrosine kinases as well as a viral kinase that, at least in the animal model provided by MHV-68, has been shown to be required for productive viral replication *in vivo*. Of these three drugs, dasatinib also showed efficacy against a KSHV-induced tumor in a mouse model and may therefore represent a candidate for drug repurposing to be evaluated in clinical trials of KSHV-associated disease.

MATERIALS AND METHODS

Cell culture, transfection, virus production. HEK293, Vero (84), Vero-rKSHV.219 (85), BJAB (86), BJAB-rKSHV.219 (50, 85), HuARLT (87), and HuARLT-rKSHV.219 (synonym, HuAR2T and HuAR2T-KSHV) cells (88, 89), SLK cells (90, 91), and iSLK cells were cultured as described previously. The production of the recombinant baculovirus expressing KSHV ORF50/RTA used to trigger lytic reactivation was described previously (85). HEK293 cells were transfected in six-well plates with 1 μg of each construct using the FuGENE transfection reagent (Promega) at a ratio 3 μl:1 μg of DNA and harvested 48 h after transfection.

An rKSHV.219 virus stock was produced from BJAB cells infected with rKSHV.219 as previously described (92). iSLK cells stably transfected with KSHV BAC16 WT or the 3GV mutant were induced with Na butyrate (SB; 2 mM) and doxycycline (2 μg/ml). To determine the titer of the virus produced by iSLK/BACs or BJAB-rKSHV.219, the supernatant collected 48 h after reactivation/treatment was used to infect HEK293 cells in a 96-well plate (3×10^4 cells/well). The plate was centrifuged for 30 min at 32°C and 450 $\times$ *g*. Seventy-two hours later, infected GFP-positive HEK293 cells were counted and the viral titer was calculated.

Mutagenesis of KSHV BAC16 and generation of KSHV BAC16 stable cell lines. The following primers were used to insert three point mutations ($G_{260}V$, $G_{263}V$, $G_{265}V$) into the ATP binding pocket of the ORF21 gene in the KSHV genome following the "En passant" protocol: 5′-ACC GTG GAC TAC AGG AAT GTT TAT TTG CTT TAC TTA GAG GTG GTA ATG GTT GTG GTC AAA TCA ACG CTG GTC AAC GGA CGC ATC GTG GCC GGA TCT C-3′ and 5′-GGG CAA GAT CCC GCA CAC GGC GTT GAC CAG CGT TGA TTT GAC CAC AAC CAT TAC CAC CTC TAA GTA AAG CAA ATA AGT GAC CAC GTC GTG GAA TGC-3′ (93). This mutant was named KSHV BAC16 3GV. Two individual clones from the first recombination step were selected and used for the second recombination step. New KSHV BAC16 constructs were confirmed by enzymatic digestion and completely sequenced on an Illumina MiSeq sequencer. To generate stable iSLK/BAC16 cells, iSLK cells were transfected with the KSHV BAC16 WT or BAC16 3GV mutant DNA using Fugene 6 (Roche no. 11814443001) and selected with 1.2 mg/ml hygromycin B for 2 to 3 weeks and maintained as a polyclonal culture with 100 μg/ml hygromycin B (94).

Expression plasmid. GFP-TK was obtained by cloning KSHV ORF21 in the pEGFP-C2 vector (Clontech). ORF21 was amplified by PCR from KSHV WT BAC16 using the following primers: 5′-CAC CTC GAG AGC AGA AGG CGG TTT TG-3′, which contains a XhoI restriction site, and 5′-GCC GAA TTC CTA GAC CCT GCA TGT CTC CTC-3′, which contains an EcoRI site. The amplified product and pEGFP-C2 were digested by EcoRI and XhoI prior to ligation.

A GFP-TK 3GV mutant containing three point mutations ($G_{260}V$, $G_{263}V$, $G_{265}V$) in the ATP binding site was generated by PCR-based mutagenesis using the following primers: 5′-GCT TTA CTT AGA GGT GGT AAT GGT TGT GGT CAA ATC AAC GCT GGT CAA C-3′ and 5′-GTT GAC CAG CGT TGA TTT GAC CAC AAC CAT TAC CAC CTC TAA GTA AAG C-3′. A mutant with three mutations of tyrosine residues in GFP-TK ($Y_{65}F$, $Y_{85}F$, $Y_{120}F$) was also generated by PCR-based mutagenesis using the primers for $Y_{65}F$ (5′-CCT CGT ACA TAT TCG ACG TGC CCA CCG-3′; 5′-CGG TGG GCA CGT CGA ATA TGT ACG AGG-3′), $Y_{85}F$ (5′-TGC ACG ACA ACT CCC TCT TTG CAA CGC CTA GGT TTC CGC C-3′; 5′-GGC GGA AAC CTA GGC GTT GCA AAG AGG GAG TTG TCG TGC A-3′), and $Y_{120}F$ (5′-TGA CGA CGA CTC GGG AGA CTT TGC GCC AAT GGA TCG CTT C-3′; 5′-GAA GCG ATC CAT TGG CGC AAA GTC TCC GAG TCG TCG TCA-3′). The presence of the correct mutation and the absence of unintended mutations were checked by Sanger sequencing.

Immunoblotting, antibodies, immunoprecipitation, kinase assay. For immunoblotting, cells were lysed in SDS sample buffer (62.5 mM Tris-HCl, pH 6.8, 2% [wt/vol] SDS, 10% glycerol, 50 mM dithiothreitol [DTT], 0.01% [wt/vol] bromophenol blue) and immunoblot analyses were performed using standard protocols. Proteins were detected using the following primary antibodies: mouse monoclonal HHV-8 K-bZIP antibody F33P1 (sc-69797; Santa Cruz), mouse monoclonal KSHV ORF45 antibody (sc-53883; Santa Cruz), rat monoclonal KSHV ORF73 (LNA-1) antibody (13-210-100; Advanced Biotechnologies), rabbit monoclonal GAPDH antibody (no. 2118; Cell Signaling Technology), mouse monoclonal β-actin antibody (no. A5441; Sigma), mouse monoclonal phosphotyrosine antibody (P-Tyr-100) (Cell Signaling Technology), mouse monoclonal GFP antibody (no. 632380; Clontech), and rabbit polyclonal GFP antibody (no. 632592; Clontech).

For immunoprecipitation of GFP-tagged ORF21/TK, HEK293 cells were collected 48 h after transfection and lysed for 1 h on ice with lysis buffer (10 mM Tris-HCl, pH 7.4, 150 mM NaCl, 5 mM EDTA, 10% glycerol, 1% Triton X-100) supplemented with cOmplete Ultra protease inhibitor cocktail (Roche) and PhosSTOP phosphatase inhibitor cocktail (Roche). Lysates were centrifuged at 20,000 $\times$ *g* at 4°C for 10 min, and the resulting supernatants were gently shaken overnight at 4°C with protein G Sepharose 4 fast flow beads (GE Healthcare) and rabbit polyclonal GFP antibody (no. 632592; Clontech) diluted to 1/500. The beads were washed three times with lysis buffer and analyzed by SDS-PAGE and immunoblotting. A similar protocol was used for immunoprecipitation of induced/treated iSLK/KSHV BAC16 WT and iSLK/KSHV BAC16 3GV cells.

For the kinase assay, beads obtained after immunoprecipitation of GFP-TK were washed twice with lysis buffer, followed by a single wash with 25 mM HEPES, pH 7, 50 mM NaCl, 2.5 mM EDTA, and 2.5 mM DTT. Beads were incubated for 30 min at 30°C and washed with a kinase assay buffer (10 mM HEPES, pH 7.7, 75 mM NaCl, 5 mM EDTA, 0.5 mM DTT) supplemented with PhosSTOP phosphatase inhibitor cocktail (Roche). The beads were then incubated for 30 min at 30°C in the presence of 0.4 μM ATP and the FDA-approved kinase inhibitors diluted in kinase assay buffer, and the reaction was stopped with 5$\times$ SDS sample buffer (250 mM Tris-HCl, pH 6.8, 10% [wt/vol] SDS, 50% glycerol, 250 mM DTT, 0.05% [wt/vol] bromophenol blue).

Inhibition of KSHV lytic replication by kinase inhibitors and cell viability assay. For BJAB-rKSHV.219, 1.5×10^4 cells per well were plated in 384-well plates. Twenty-four hours later, cells were

treated with kinase inhibitors and triggered for lytic reactivation for 72 h as previously described (92, 95). Supernatants from BJAB-rKSHV.219 cells were collected and used to infect fresh HEK293 cells that had been seeded into a 384-well plate 24 h earlier at a density of 4×10^3 cells per well. HEK293 cells were then centrifuged for 30 min at 30°C and 450 × *g* and incubated at 37°C for 72 h. The cells were fixed with glutaraldehyde and washed with phosphate-buffered saline (PBS). *De novo* infection was evaluated by the mean fluorescence intensity of GFP-positive HEK293 cells quantified in a BioTek luminometer. HuARLT-rKSHV.219 (1.3×10^4 cells/well) or Vero-rKSHV.219 (5×10^3 cells/well) cells were plated in 96-well plates and, 24 h later, treated with kinase inhibitors and a baculovirus expressing the KSHV RTA protein and 1.25 mM Na butyrate for 48 h to activate lytic replication. Following fixation with glutaraldehyde, KSHV lytic reactivation was evaluated by quantifying the number of RFP-positive cells using CellProfiler (96).

Cell viability after inhibitor treatment was estimated using an MTT assay for BJAB-rKSHV.219 cells or DAPI staining after glutaraldehyde fixation for HuARLT-rKSHV.219 and Vero-rKSHV.219 cells. Afatinib, axitinib, bosutinib, cabozantinib, ibrutinib, lenvatinib, ponatinib, regorafenib, ruxolitinib phosphate, sorafenib, tofacitinib, vandetanib, and vemurafenib were obtained from AbMole. Dabrafenib, nintedanib, motesanib diphosphate, palbociclib, and trametinib were obtained from Selleckchem. Anhydrous dasatinib was purchased from Santa Cruz Biotechnology. Crizotinib, imatinib mesylate, and sunitinib malate were from Sigma. Ceritinib, erlotinib, gefitinib, lapatinib ditosylate, nilotinib, and pazopanib were from Chemietek. All compounds were dissolved at 20 mM in DMSO, except for erlotinib, imatinib mesylate, and palbociclib, which were dissolved in water. Erlotinib and lapatinib ditosylate were diluted to 1 mM and 5 mM, respectively. After reconstitution, the inhibitors were stored at −20°C with protection from light. Cells were treated with compounds at concentrations indicated in the figure legends, and controls contained equivalent amounts of DMSO (Applichem). DMSO concentrations did not exceed 0.1%.

iSLK cells stably transfected with KSHV BAC16 WT or 3GV were induced with SB (1 mM) and doxycycline (1 μg/ml) and treated with 0.01 μM to 10 μM dasatinib (Abmole), brivudine (Abmole), or zidovudine (Sigma). DMSO-treated nonreactivated and reactivated cells were used as controls. To determine the production of infectious viral particles, the cell culture supernatants of the iSLK cell lines were centrifuged for 5 min at 2,500 rpm at 4°C and added to 3×10^4 HEK293 cells in a 96-well plate, which had been seeded the day before. The plate was centrifuged for 30 min at 32°C and 450 × *g*. Forty-eight hours postinfection, cells were fixed with paraformaldehyde (PFA) and viral titers were calculated by counting GFP-positive cells per well using a Citation 5 cell imaging multimode reader from BioTek. Cell viability after inhibitor treatment was estimated using an MTT assay 48 h posttreatment.

Entry assay on HEK293. HEK293 cells were infected with rKSHV.219 (multiplicity of infection [MOI], 1) and treated with 1 μM and 10 μM inhibitors. The plate was centrifuged for 30 min at 32°C and 450 × *g*. Forty-eight hours after infection and treatment, cells were fixed with PFA, and the infected GFP-positive cells were counted using a Citation 5 cell imaging multi-mode reader from BioTek.

Implantation of HuARLT-rKSHV cells in mice. HuARLT-rKSHV cells were transplanted into mice as described previously (89). A total of 1.2×10^6 cells were seeded into each well of AggreWell 400 (27945; Stemcell Technologies), centrifuged for 3 min at 100 × *g*, and cultivated for 3 days at 37°C. Four hundred spheroids were used for each Matrigel implant containing 0.2% methylcellulose (M0512; Sigma), 3 mg/ml fibrinogen (341576; Calbiochem), EGM medium (CC-3124; Lonza), 10 μg/ml fibroblast growth factor (FGF) (100-18B-250; PeproTech), 0.5 μg/ml VEGF (RCPG246; Randox), 1 U/liter thrombin (605190-100U; Merck Millipore), and 300 μl of Matrigel HC, growth factor reduced (354263; Corning). The mixture was injected subcutaneously into Rag2$^{-/-}$ γc$^{-/-}$ mice. Starting from day 1 after implantation, the mice were treated with dasatinib (30 mg/kg), ibrutinib (50 mg/kg), imatinib (100 mg/kg), or ponatinib (30 mg/kg) by oral gavage 6 times a week. Rapamycin (2 mg/kg) was injected intraperitoneally 3 times a week. After 4 weeks of treatment, Matrigel implants were extracted and fixed with 4% formalin. The diameters of the lesions were measured on sections stained for human vimentin.

Animal experiments were performed in accordance with the local authorities (Lower Saxony Veterinary Office permission/license number 33.19-42502-04-17/2480).

Statistical tests. One-way analysis of variance (ANOVA), followed by Dunnett's multiple-comparison test and unpaired *t* test were performed using GraphPad Prism version 5.00 for Windows (GraphPad Software, La Jolla, CA, USA).

Data availability. The sequence of the KSHV BAC16 3GV mutant was deposited in GenBank under accession number MN752405.

ACKNOWLEDGMENTS

G.B. and T.F.S. conceived the study and wrote the manuscript. D.W. and T.D. planned the animal experiments. G.B., E.N., T.D., J.R., and S.K. carried out the experiments. A.D. performed NGS sequencing and analysis. All authors reviewed and approved the manuscript.

We thank Elias Hage and Aurélie Ducroux for critical reading of the manuscript and Aurélie Ducroux, Naira Samarina, and all lab members for help and discussions.

This work was supported by the German Centre of Infection Research (DZIF), Thematic Translational Unit Infections of the Immunocompromised Host (project 07.802; to T.F.S.), the Deutsche Forschungsgemeinschaft through the Cluster of Excellence 2155 RESIST, and the Fondation Ernst & Margarete Wagemann (to G.B.).

The funders had no role in the design or execution of the study nor in the decision to submit the work for publication.

REFERENCES

1. Ferlay J, Soerjomataram I, Ervik M, Dikshit R, Eser S, Mathers C, Rebelo M, Parkin DM, Forman D, Bray F. 2013. GLOBOCAN 2012 v1.0, Cancer incidence and mortality worldwide: IARC cancer base no. 11. International Agency for Research on Cancer, Lyon, France.
2. Rohner E, Wyss N, Trelle S, Mbulaiteye SM, Egger M, Novak U, Zwahlen M, Bohlius J. 2014. HHV-8 seroprevalence: a global view. Syst Rev 3:11. https://doi.org/10.1186/2046-4053-3-11.
3. Ganem D. 2007. KSHV-induced oncogenesis, p. 1007–1028. *In* Arvin A, Campadelli-Fiume G, Mocarski E, et al (ed), Human herpesviruses: biology, therapy, and immunoprophylaxis. Cambridge University Press, Cambridge, United Kingdom.
4. Cai Q, Lan K, Verma SC, Si H, Lin D, Robertson ES. 2006. Kaposi's sarcoma-associated herpesvirus latent protein LANA interacts with HIF-1 to upregulate RTA expression during hypoxia: latency control under low oxygen conditions. J Virol 80:7965–7975. https://doi.org/10.1128/JVI.00689-06.
5. Cai Q, Cai S, Zhu C, Verma SC, Choi J-Y, Robertson ES. 2013. A unique SUMO-2-interacting motif within LANA is essential for KSHV latency. PLoS Pathog 9:e1003750. https://doi.org/10.1371/journal.ppat.1003750.
6. Zhang L, Zhu C, Guo Y, Wei F, Lu J, Qin J, Banerjee S, Wang J, Shang H, Verma SC, Yuan Z, Robertson ES, Cai Q. 2014. Inhibition of KAP1 enhances hypoxia-induced Kaposi's sarcoma-associated herpesvirus reactivation through RBP-J. J Virol 88:6873–6884. https://doi.org/10.1128/JVI.00283-14.
7. Ye F, Zhou F, Bedolla RG, Jones T, Lei X, Kang T, Guadalupe M, Gao S-J. 2011. Reactive oxygen species hydrogen peroxide mediates Kaposi's sarcoma-associated herpesvirus reactivation from latency. PLoS Pathog 7:e1002054. https://doi.org/10.1371/journal.ppat.1002054.
8. Krishnan HH, Naranatt PP, Smith MS, Zeng L, Bloomer C, Chandran B. 2004. Concurrent expression of latent and a limited number of lytic genes with immune modulation and antiapoptotic function by Kaposi's sarcoma-associated herpesvirus early during infection of primary endothelial and fibroblast cells and subsequent decline of lytic gene expression. J Virol 78:3601–3620. https://doi.org/10.1128/jvi.78.7.3601-3620.2004.
9. Parravicini C, Corbellino M, Paulli M, Magrini U, Lazzarino M, Moore PS, Chang Y. 1997. Expression of a virus-derived cytokine, KSHV vIL-6, in HIV-seronegative Castleman's disease. Am J Pathol 151:1517–1522.
10. Jones KD, Aoki Y, Chang Y, Moore PS, Yarchoan R, Tosato G. 1999. Involvement of interleukin-10 (IL-10) and viral IL-6 in the spontaneous growth of Kaposi's sarcoma herpesvirus-associated infected primary effusion lymphoma cells. Blood 94:2871–2879. https://doi.org/10.1182/blood.V94.8.2871.
11. Parravicini C, Chandran B, Corbellino M, Berti E, Paulli M, Moore PS, Chang Y. 2000. Differential viral protein expression in Kaposi's sarcoma-associated herpesvirus-infected diseases: Kaposi's sarcoma, primary effusion lymphoma, and multicentric Castleman's disease. Am J Pathol 156:743–749. https://doi.org/10.1016/S0002-9440(10)64940-1.
12. Ma T, Jham BC, Hu J, Friedman ER, Basile JR, Molinolo A, Sodhi A, Montaner S. 2010. Viral G protein-coupled receptor up-regulates angiopoietin-like 4 promoting angiogenesis and vascular permeability in Kaposi's sarcoma. Proc Natl Acad Sci U S A 107:14363–14368. https://doi.org/10.1073/pnas.1001065107.
13. Uldrick TS, Wang V, O'Mahony D, Aleman K, Wyvill KM, Marshall V, Steinberg SM, Pittaluga S, Maric I, Whitby D, Tosato G, Little RF, Yarchoan R. 2010. An interleukin-6-related systemic inflammatory syndrome in patients co-infected with Kaposi sarcoma-associated herpesvirus and HIV but without multicentric Castleman. Clin Infect Dis 51:350–358. https://doi.org/10.1086/654798.
14. Moore PS, Boshoff C, Weiss RA, Chang Y. 1996. Molecular mimicry of human cytokine and cytokine response pathway genes by KSHV. Science 274:1739–1744. https://doi.org/10.1126/science.274.5293.1739.
15. Chen L, Lagunoff M. 2005. Establishment and maintenance of Kaposi's sarcoma-associated herpesvirus latency in B cells. J Virol 79:14383–14391. https://doi.org/10.1128/JVI.79.22.14383-14391.2005.
16. Aoki Y, Jaffe ES, Chang Y, Jones K, Teruya-Feldstein J, Moore PS, Tosato G. 1999. Angiogenesis and hematopoiesis induced by Kaposi's sarcoma-associated herpesvirus-encoded interleukin-6. Blood 93:4034–4043. https://doi.org/10.1182/blood.V93.12.4034.412k38_4034_4043.
17. Meads MB, Medveczky PG. 2004. Kaposi's sarcoma-associated herpesvirus-encoded viral interleukin-6 is secreted and modified differently than human interleukin-6: evidence for a unique autocrine signaling mechanism. J Biol Chem 279:51793–51803. https://doi.org/10.1074/jbc.M407382200.
18. Guo H-G, Browning P, Nicholas J, Hayward GS, Tschachler E, Jiang Y-W, Sadowska M, Raffeld M, Colombini S, Gallo RC, Reitz MS. 1997. Characterization of a chemokine receptor-related gene in human herpesvirus 8 and its expression in Kaposi's sarcoma. Virology 228:371–378. https://doi.org/10.1006/viro.1996.8386.
19. Chiou C-J, Poole LJ, Kim PS, Ciufo DM, Cannon JS, Ap Rhys CM, Alcendor DJ, Zong J-C, Ambinder RF, Hayward GS. 2002. Patterns of gene expression and a transactivation function exhibited by the vGCR (ORF74) chemokine receptor protein of Kaposi's sarcoma-associated herpesvirus. J Virol 76:3421–3439. https://doi.org/10.1128/jvi.76.7.3421-3439.2002.
20. Arvanitakis L, Geras-Raaka E, Varma A, Gershengorn MC, Cesarman E. 1997. Human herpesvirus KSHV encodes a constitutively active G-protein-coupled receptor linked to cell proliferation. Nature 385:347–350. https://doi.org/10.1038/385347a0.
21. Neipel F, Albrecht JC, Ensser A, Huang YQ, Li JJ, Friedman-Kien AE, Fleckenstein B. 1997. Human herpesvirus 8 encodes a homolog of interleukin-6. J Virol 71:839–842.
22. Nicholas J, Ruvolo VR, Burns WH, Sandford G, Wan X, Ciufo D, Hendrickson SB, Guo HG, Hayward GS, Reitz MS. 1997. Kaposi's sarcoma-associated human herpesvirus-8 encodes homologues of macrophage inflammatory protein-1 and interleukin-6. Nat Med 3:287–292. https://doi.org/10.1038/nm0397-287.
23. Mori Y, Nishimoto N, Ohno M, Inagi R, Dhepakson P, Amou K, Yoshizaki K, Yamanishi K. 2000. Human herpesvirus 8-encoded interleukin-6 homologue (viral IL-6) induces endogenous human IL-6 secretion. J Med Virol 61:332–335. https://doi.org/10.1002/1096-9071(200007)61:3<332::aid-jmv8>3.0.co;2-3.
24. Foussat A, Wijdenes J, Bouchet L, Gaidano G, Neipel F, Balabanian K, Galanaud P, Couderc J, Emilie D. 1999. Human interleukin-6 is in vivo an autocrine growth factor for human herpesvirus-8-infected malignant B lymphocytes. Eur Cytokine Netw 10:501–508.
25. Stine JT, Wood C, Hill M, Epp A, Raport CJ, Schweickart VL, Endo Y, Sasaki T, Simmons G, Boshoff C, Clapham P, Chang Y, Moore P, Gray PW, Chantry D. 2000. KSHV-encoded CC chemokine vMIP-III is a CCR4 agonist, stimulates angiogenesis, and selectively chemoattracts TH2 cells. Blood 95:1151–1157. https://doi.org/10.1182/blood.V95.4.1151.004k37_1151_1157.
26. Wen KW, Damania B. 2010. Hsp90 and Hsp40/Erdj3 are required for the expression and anti-apoptotic function of KSHV K1. Oncogene 29:3532–3544. https://doi.org/10.1038/onc.2010.124.
27. Sun R, Lin SF, Staskus K, Gradoville L, Grogan E, Haase A, Miller G. 1999. Kinetics of Kaposi's sarcoma-associated herpesvirus gene expression. J Virol 73:2232–2242.
28. Brinkmann MM, Pietrek M, Dittrich-Breiholz O, Kracht M, Schulz TF. 2007. Modulation of host gene expression by the K15 protein of Kaposi's sarcoma-associated herpesvirus. J Virol 81:42–58. https://doi.org/10.1128/JVI.00648-06.
29. Wang L, Brinkmann MM, Pietrek M, Ottinger M, Dittrich-Breiholz O, Kracht M, Schulz TF. 2007. Functional characterization of the M-type K15-encoded membrane protein of Kaposi's sarcoma-associated herpesvirus. J Gen Virol 88:1698–1707. https://doi.org/10.1099/vir.0.82807-0.
30. Glenn M, Rainbow L, Auradé F, Davison A, Schulz TF. 1999. Identification of a spliced gene from Kaposi's sarcoma-associated herpesvirus encoding a protein with similarities to latent membrane proteins 1 and 2A of Epstein-Barr virus. J Virol 73:6953–6963.
31. Brinkmann MM, Glenn M, Rainbow L, Kieser A, Henke-Gendo C, Schulz TF. 2003. Activation of mitogen-activated protein kinase and NF-kappaB pathways by a Kaposi's sarcoma-associated herpesvirus K15 membrane protein. J Virol 77:9346–9358. https://doi.org/10.1128/jvi.77.17.9346-9358.2003.

32. Cesarman E, Nador RG, Bai F, Bohenzky RA, Russo JJ, Moore PS, Chang Y, Knowles DM. 1996. Kaposi's sarcoma-associated herpesvirus contains G protein-coupled receptor and cyclin D homologs which are expressed in Kaposi's sarcoma and malignant lymphoma. J Virol 70:8218–8223.
33. Haque M, Davis DA, Wang V, Widmer I, Yarchoan R. 2003. Kaposi's sarcoma-associated herpesvirus (human herpesvirus 8) contains hypoxia response elements: relevance to lytic induction by hypoxia. J Virol 77:6761–6768. https://doi.org/10.1128/jvi.77.12.6761-6768.2003.
34. Haque M, Wang V, Davis DA, Zheng Z-M, Yarchoan R. 2006. Genetic organization and hypoxic activation of the Kaposi's sarcoma-associated herpesvirus ORF34-37 gene cluster. J Virol 80:7037–7051. https://doi.org/10.1128/JVI.00553-06.
35. Lai I-C, Farrell PJ, Kellam P. 2011. X-box binding protein 1 induces the expression of the lytic cycle transactivator of Kaposi's sarcoma-associated herpesvirus but not Epstein-Barr virus in co-infected primary effusion lymphoma. J Gen Virol 92:421–431. https://doi.org/10.1099/vir.0.025494-0.
36. Hu D, Wang V, Yang M, Abdullah S, Davis DA, Uldrick TS, Polizzotto MN, Veeranna RP, Pittaluga S, Tosato G, Yarchoan R. 2016. Induction of Kaposi's sarcoma-associated herpesvirus-encoded viral interleukin-6 by X-box binding protein 1. J Virol 90:368–378. https://doi.org/10.1128/JVI.01192-15.
37. Chang P-C, Campbell M, Robertson ES. 2016. Human oncogenic herpesvirus and post-translational modifications—phosphorylation and SUMOylation. Front Microbiol 7:962. https://doi.org/10.3389/fmicb.2016.00962.
38. Coen N, Duraffour S, Snoeck R, Andrei G. 2014. KSHV targeted therapy: an update on inhibitors of viral lytic replication. Viruses 6:4731–4759. https://doi.org/10.3390/v6114731.
39. Gustafson EA, Schinazi RF, Fingeroth JD. 2000. Human herpesvirus 8 open reading frame 21 is a thymidine and thymidylate kinase of narrow substrate specificity that efficiently phosphorylates zidovudine but not ganciclovir. J Virol 74:684–692. https://doi.org/10.1128/jvi.74.2.684-692.2000.
40. Coen N, Duraffour S, Topalis D, Snoeck R, Andrei G. 2014. Spectrum of activity and mechanisms of resistance of various nucleoside derivatives against gammaherpesviruses. Antimicrob Agents Chemother 58:7312–7323. https://doi.org/10.1128/AAC.03957-14.
41. Casper C, Nichols WG, Huang M-L, Corey L, Wald A. 2004. Remission of HHV-8 and HIV-associated multicentric Castleman disease with ganciclovir treatment. Blood 103:1632–1634. https://doi.org/10.1182/blood-2003-05-1721.
42. Uldrick TS, Polizzotto MN, Aleman K, O'Mahony D, Wyvill KM, Wang V, Marshall V, Pittaluga S, Steinberg SM, Tosato G, Whitby D, Little RF, Yarchoan R. 2011. High-dose zidovudine plus valganciclovir for Kaposi sarcoma herpesvirus-associated multicentric Castleman disease: a pilot study of virus-activated cytotoxic therapy. Blood 117:6977–6986. https://doi.org/10.1182/blood-2010-11-317610.
43. Gill MB, Turner R, Stevenson PG, Way M. 2015. KSHV-TK is a tyrosine kinase that disrupts focal adhesions and induces Rho-mediated cell contraction. EMBO J 34:448–465. https://doi.org/10.15252/embj.201490358.
44. Gill MB, Murphy J-E, Fingeroth JD. 2005. Functional divergence of Kaposi's sarcoma-associated herpesvirus and related gamma-2 herpesvirus thymidine kinases: novel cytoplasmic phosphoproteins that alter cellular morphology and disrupt adhesion. J Virol 79:14647–14659. https://doi.org/10.1128/JVI.79.23.14647-14659.2005.
45. Gill MB, Wright DE, Smith CM, May JS, Stevenson PG. 2009. Murid herpesvirus-4 lacking thymidine kinase reveals route-dependent requirements for host colonization. J Gen Virol 90:1461–1470. https://doi.org/10.1099/vir.0.010603-0.
46. Coen DM, Kosz-Vnenchak M, Jacobson JG, Leib DA, Bogard CL, Schaffer PA, Tyler KL, Knipe DM. 1989. Thymidine kinase-negative herpes simplex virus mutants establish latency in mouse trigeminal ganglia but do not reactivate. Proc Natl Acad Sci U S A 86:4736–4740. https://doi.org/10.1073/pnas.86.12.4736.
47. Coleman HM, de Lima B, Morton V, Stevenson PG. 2003. Murine gammaherpesvirus 68 lacking thymidine kinase shows severe attenuation of lytic cycle replication in vivo but still establishes latency. J Virol 77:2410–2417. https://doi.org/10.1128/jvi.77.4.2410-2417.2003.
48. Song MJ, Hwang S, Wong WH, Wu T-T, Lee S, Liao H-I, Sun R. 2005. Identification of viral genes essential for replication of murine gammaherpesvirus 68 using signature-tagged mutagenesis. Proc Natl Acad Sci U S A 102:3805–3810. https://doi.org/10.1073/pnas.0404521102.
49. Pepper SD, Stewart JP, Arrand JR, Mackett M. 1996. Murine gammaherpesvirus-68 encodes homologues of thymidine kinase and glycoprotein H: sequence, expression, and characterization of pyrimidine kinase activity. Virology 219:475–479. https://doi.org/10.1006/viro.1996.0274.
50. Kati S, Tsao EH, Günther T, Weidner-Glunde M, Rothämel T, Grundhoff A, Kellam P, Schulz TF. 2013. Activation of the B cell antigen receptor triggers reactivation of latent Kaposi's sarcoma-associated herpesvirus in B cells. J Virol 87:8004–8016. https://doi.org/10.1128/JVI.00506-13.
51. Dubich T, Lieske A, Santag S, Beauclair G, Rückert J, Herrmann J, Gorges J, Büsche G, Kazmaier U, Hauser H, Stadler M, Schulz TF, Wirth D. 2019. An endothelial cell line infected by Kaposi's sarcoma–associated herpes virus (KSHV) allows the investigation of Kaposi's sarcoma and the validation of novel viral inhibitors in vitro and in vivo. J Mol Med (Berl) 97:311–324. https://doi.org/10.1007/s00109-018-01733-1.
52. Campbell TB, Borok M, Gwanzura L, MaWhinney S, White IE, Ndemera B, Gudza I, Fitzpatrick L, Schooley RT. 2000. Relationship of human herpesvirus 8 peripheral blood virus load and Kaposi's sarcoma clinical stage. AIDS 14:2109–2116. https://doi.org/10.1097/00002030-200009290-00006.
53. Boneschi V, Brambilla L, Berti E, Ferrucci S, Corbellino M, Parravicini C, Fossati S. 2001. Human herpesvirus 8 DNA in the skin and blood of patients with Mediterranean Kaposi's sarcoma: clinical correlations. Dermatology 203:19–23. https://doi.org/10.1159/000051697.
54. Oksenhendler E, Carcelain G, Aoki Y, Boulanger E, Maillard A, Clauvel JP, Agbalika F. 2000. High levels of human herpesvirus 8 viral load, human interleukin-6, interleukin-10, and C reactive protein correlate with exacerbation of multicentric Castleman disease in HIV-infected patients. Blood 96:2069–2073. https://doi.org/10.1182/blood.V96.6.2069.
55. Grandadam M, Dupin N, Calvez V, Gorin I, Blum L, Kernbaum S, Sicard D, Buisson Y, Agut H, Escande JP, Huraux JM. 1997. Exacerbations of clinical symptoms in human immunodeficiency virus type 1-infected patients with multicentric Castleman's disease are associated with a high increase in Kaposi's sarcoma herpesvirus DNA load in peripheral blood mononuclear cells. J Infect Dis 175:1198–1201. https://doi.org/10.1086/593567.
56. Polizzotto MN, Uldrick TS, Hu D, Yarchoan R. 2012. Clinical manifestations of Kaposi sarcoma herpesvirus lytic activation: multicentric Castleman disease (KSHV-MCD) and the KSHV inflammatory cytokine syndrome. Front Microbiol 3:73. https://doi.org/10.3389/fmicb.2012.00073.
57. Koon HB, Bubley GJ, Pantanowitz L, Masiello D, Smith B, Crosby K, Proper JA, Weeden W, Miller TE, Chatis P, Egorin MJ, Tahan SR, Dezube BJ. 2005. Imatinib-induced regression of AIDS-related Kaposi's. J Clin Oncol 23:982–989. https://doi.org/10.1200/JCO.2005.06.079.
58. Koon HB, Krown SE, Lee JY, Honda K, Rapisuwon S, Wang Z, Aboulafia D, Reid EG, Rudek MA, Dezube BJ, Noy A. 2014. Phase II trial of imatinib in AIDS-associated Kaposi's sarcoma: AIDS malignancy consortium protocol 042. J Clin Oncol 32:402–408. https://doi.org/10.1200/JCO.2012.48.6365.
59. Douglas JL, Whitford JG, Moses AV. 2009. Characterization of c-Kit expression and activation in KSHV-infected endothelial cells. Virology 390:174–185. https://doi.org/10.1016/j.virol.2009.05.011.
60. Moses AV, Jarvis MA, Raggo C, Bell YC, Ruhl R, Luukkonen BGM, Griffith DJ, Wait CL, Druker BJ, Heinrich MC, Nelson JA, Früh K. 2002. Kaposi's sarcoma-associated herpesvirus-induced upregulation of the c-kit proto-oncogene, as identified by gene expression profiling, is essential for the transformation of endothelial cells. J Virol 76:8383–8399. https://doi.org/10.1128/jvi.76.16.8383-8399.2002.
61. Davis MI, Hunt JP, Herrgard S, Ciceri P, Wodicka LM, Pallares G, Hocker M, Treiber DK, Zarrinkar PP. 2011. Comprehensive analysis of kinase inhibitor selectivity. Nat Biotechnol 29:1046–1051. https://doi.org/10.1038/nbt.1990.
62. Santos FPS, Ravandi F. 2009. Advances in treatment of chronic myelogenous leukemia—new treatment options with tyrosine kinase inhibitors. Leuk Lymphoma 50(Suppl 2):16–26. https://doi.org/10.3109/10428190903383427.
63. Lagunoff M, Lukac DM, Ganem D. 2001. Immunoreceptor tyrosine-based activation motif-dependent signaling by Kaposi's sarcoma-associated herpesvirus K1 protein: effects on lytic viral replication. J Virol 75:5891–5898. https://doi.org/10.1128/JVI.75.13.5891-5898.2001.
64. Prakash O, Swamy OR, Peng X, Tang Z-Y, Li L, Larson JE, Cohen JC, Gill J, Farr G, Wang S, Samaniego F. 2005. Activation of Src kinase Lyn by the Kaposi sarcoma-associated herpesvirus K1 protein: implications for lymphomagenesis. Blood 105:3987–3994. https://doi.org/10.1182/blood-2004-07-2781.

65. Qin D, Feng N, Fan W, Ma X, Yan Q, Lv Z, Zeng Y, Zhu J, Lu C, McLemore M, Grewal S, Liu F, Archambault A, Poursine-Laurent J, Haug J, Link D, Zhou C, Saxon A, Zhang K, Fang J, Ding M, Yang L, Liu L, Jiang B, Huang L, Chao M, Chen M, Shih H, Chiang Y, Chuang C, Lee C, Lei X, Bai Z, Ye F, Xie J, Kim C, Huang Y, Gao S, Finbloom D, Winestock K, Kelly-Welch A, Hanson E, Boothby M, Keegan A, Deng J, Hua K, Lesser S, Greiner A, Walter A, Marrero M, et al. 2011. Activation of PI3K/AKT and ERK MAPK signal pathways is required for the induction of lytic cycle replication of Kaposi's Sarcoma-associated herpesvirus by herpes simplex virus type 1. BMC Microbiol 11:240. https://doi.org/10.1186/1471-2180-11-240.
66. Hahn AS, Desrosiers RC. 2013. Rhesus monkey rhadinovirus uses eph family receptors for entry into B cells and endothelial cells but not fibroblasts. PLoS Pathog 9:e1003360. https://doi.org/10.1371/journal.ppat.1003360.
67. Hahn AS, Kaufmann JK, Wies E, Naschberger E, Panteleev-Ivlev J, Schmidt K, Holzer A, Schmidt M, Chen J, König S, Ensser A, Myoung J, Brockmeyer NH, Stürzl M, Fleckenstein B, Neipel F. 2012. The ephrin receptor tyrosine kinase A2 is a cellular receptor for Kaposi's sarcoma–associated herpesvirus. Nat Med 18:961–966. https://doi.org/10.1038/nm.2805.
68. Dutta D, Chakraborty S, Bandyopadhyay C, Valiya Veettil M, Ansari MA, Singh VV, Chandran B. 2013. EphrinA2 regulates clathrin mediated KSHV endocytosis in fibroblast cells by coordinating integrin-associated signaling and c-Cbl directed polyubiquitination. PLoS Pathog 9:e1003510. https://doi.org/10.1371/journal.ppat.1003510.
69. Chakraborty S, Veettil MV, Bottero V, Chandran B. 2012. Kaposi's sarcoma-associated herpesvirus interacts with EphrinA2 receptor to amplify signaling essential for productive infection. Proc Natl Acad Sci U S A 109:E1163–72. https://doi.org/10.1073/pnas.1119592109.
70. Valent P, Hadzijusufovic E, Schernthaner G-H, Wolf D, Rea D, Le Coutre P. 2015. Vascular safety issues in CML patients treated with BCR/ABL1 kinase inhibitors. Blood 125:901. https://doi.org/10.1182/blood-2014-09-594432.
71. Dillon PJ, Gregory SM, Tamburro K, Sanders MK, Johnson GL, Raab-Traub N, Dittmer DP, Damania B. 2013. Tousled-like kinases modulate reactivation of gammaherpesviruses from latency. Cell Host Microbe 13:204–214. https://doi.org/10.1016/j.chom.2012.12.005.
72. Advani RH, Buggy JJ, Sharman JP, Smith SM, Boyd TE, Grant B, Kolibaba KS, Furman RR, Rodriguez S, Chang BY, Sukbuntherng J, Izumi R, Hamdy A, Hedrick E, Fowler NH. 2013. Bruton tyrosine kinase inhibitor ibrutinib (PCI-32765) has significant activity in patients with relapsed/refractory B-cell malignancies. J Clin Oncol 31:88–94. https://doi.org/10.1200/JCO.2012.42.7906.
73. Michaelis M, Paulus C, Löschmann N, Dauth S, Stange E, Doerr HW, Nevels M, Cinatl J. 2011. The multi-targeted kinase inhibitor sorafenib inhibits human cytomegalovirus replication. Cell Mol Life Sci 68:1079–1090. https://doi.org/10.1007/s00018-010-0510-8.
74. Stallone G, Infante B, Schena A, Battaglia M, Ditonno P, Loverre A, Gesualdo L, Schena FP, Grandaliano G. 2005. Rapamycin for treatment of chronic allograft nephropathy in renal transplant patients. J Am Soc Nephrol 16:3755–3762. https://doi.org/10.1681/ASN.2005060635.
75. Yaich S, Charfeddine K, Zaghdane S, El Aoud N, Jarraya F, Kharrat M, Hachicha J. 2012. Sirolimus for the treatment of Kaposi sarcoma after renal transplantation: a series of 10 cases. Transplant Proc 44:2824–2826. https://doi.org/10.1016/j.transproceed.2012.09.025.
76. Martin DF, Kuppermann BD, Wolitz RA, Palestine AG, Li H, Robinson CA. 1999. Oral ganciclovir for patients with cytomegalovirus retinitis treated with a ganciclovir implant. Roche Ganciclovir Study Group. N Engl J Med 340:1063–1070. https://doi.org/10.1056/NEJM199904083401402.
77. Jochmann R, Lorenz P, Chudasama P, Zietz C, Stürzl M, Konrad A. 2012. KSHV paracrine effects on tumorigenesis, Herpesviridae—a look into this unique family of viruses. InTech Open https://www.intechopen.com/books/herpesviridae-a-look-into-this-unique-family-of-viruses/kshv-paracrine-effects-on-tumorigenesis.
78. Damania B. 2004. Oncogenic gamma-herpesviruses: comparison of viral proteins involved in tumorigenesis. Nat Rev Microbiol 2:656–668. https://doi.org/10.1038/nrmicro958.
79. Penkert RR, Kalejta RF. 2011. Tegument protein control of latent herpesvirus establishment and animation. Herpesviridae 2:3. https://doi.org/10.1186/2042-4280-2-3.
80. Gramolelli S, Schulz TF. 2015. The role of Kaposi sarcoma-associated herpesvirus in the pathogenesis of Kaposi sarcoma. J Pathol 235:368–380. https://doi.org/10.1002/path.4441.
81. Abere B, Schulz TF. 2016. KSHV non-structural membrane proteins involved in the activation of intracellular signaling pathways and the pathogenesis of Kaposi's sarcoma. Curr Opin Virol 20:11–19. https://doi.org/10.1016/j.coviro.2016.07.008.
82. Schulz TF, Cesarman E. 2015. Kaposi sarcoma-associated herpesvirus: mechanisms of oncogenesis. Curr Opin Virol 14:116–128. https://doi.org/10.1016/j.coviro.2015.08.016.
83. Abere B, Mamo TM, Hartmann S, Samarina N, Hage E, Rückert J, Hotop S-K, Büsche G, Schulz TF. 2017. The Kaposi's sarcoma-associated herpesvirus (KSHV) non-structural membrane protein K15 is required for viral lytic replication and may represent a therapeutic target. PLoS Pathog 13:e1006639. https://doi.org/10.1371/journal.ppat.1006639.
84. Simizu B, Rhim JS, Wiebenga NH. 1967. Characterization of the Tacaribe group of arboviruses. 1. Propagation and plaque assay of Tacaribe virus in a line of African green monkey kidney cells (Vero). Proc Soc Exp Biol Med 125:119–123. https://doi.org/10.3181/00379727-125-32029.
85. Vieira J, O'Hearn PM. 2004. Use of the red fluorescent protein as a marker of Kaposi's sarcoma-associated herpesvirus lytic gene expression. Virology 325:225–240. https://doi.org/10.1016/j.virol.2004.03.049.
86. Menezes J, Leibold W, Klein G, Clements G. 1975. Establishment and characterization of an Epstein-Barr virus (EBC)-negative lymphoblastoid B cell line (BJA-B) from an exceptional, EBV-genome-negative African Burkitt's lymphoma. Biomedicine 22:276–284.
87. May T, Butueva M, Bantner S, Markusic D, Seppen J, MacLeod RAF, Weich H, Hauser H, Wirth D. 2010. Synthetic gene regulation circuits for control of cell expansion. Tissue Eng Part A 16:441–452. https://doi.org/10.1089/ten.TEA.2009.0184.
88. Alkharsah KR, Singh VV, Bosco R, Santag S, Grundhoff A, Konrad A, Stürzl M, Wirth D, Dittrich-Breiholz O, Kracht M, Schulz TF. 2011. Deletion of Kaposi's sarcoma-associated herpesvirus FLICE inhibitory protein, vFLIP, from the viral genome compromises the activation of STAT1-responsive cellular genes and spindle cell formation in endothelial cells. J Virol 85:10375–10388. https://doi.org/10.1128/JVI.00226-11.
89. Lipps C, Badar M, Butueva M, Dubich T, Singh VV, Rau S, Weber A, Kracht M, Köster M, May T, Schulz TF, Hauser H, Wirth D. 2017. Proliferation status defines functional properties of endothelial cells. Cell Mol Life Sci 74:1319–1333. https://doi.org/10.1007/s00018-016-2417-5.
90. Stürzl M, Gaus D, Dirks WG, Ganem D, Jochmann R. 2013. Kaposi's sarcoma-derived cell line SLK is not of endothelial origin, but is a contaminant from a known renal carcinoma cell line. Int J Cancer 132:1954–1958. https://doi.org/10.1002/ijc.27849.
91. Siegal B, Levinton-Kriss S, Schiffer A, Sayar J, Engelberg I, Vonsover A, Ramon Y, Rubinstein E. 1990. Kaposi's sarcoma in immunosuppression. Possibly the result of a dual viral infection. Cancer 65:492–498. https://doi.org/10.1002/1097-0142(19900201)65:3<492::AID-CNCR2820650320>3.0.CO;2-C.
92. Kati S, Hage E, Mynarek M, Ganzenmueller T, Indenbirken D, Grundhoff A, Schulz TF. 2015. Generation of high-titre virus stocks using BrK.219, a B-cell line infected stably with recombinant Kaposi's sarcoma-associated herpesvirus. J Virol Methods 217:79–86. https://doi.org/10.1016/j.jviromet.2015.02.022.
93. Tischer BK, Smith GA, Osterrieder N. 2010. En passant mutagenesis: a two step markerless red recombination system. Methods Mol Biol 634:421–430. https://doi.org/10.1007/978-1-60761-652-8_30.
94. Brulois KF, Chang H, Lee A-Y, Ensser A, Wong L-Y, Toth Z, Lee SH, Lee H-R, Myoung J, Ganem D, Oh T-K, Kim JF, Gao S-J, Jung JU. 2012. Construction and manipulation of a new Kaposi's sarcoma-associated herpesvirus bacterial artificial chromosome clone. J Virol 86:9708–9720. https://doi.org/10.1128/JVI.01019-12.
95. Haas DA, Bala K, Büsche G, Weidner-Glunde M, Santag S, Kati S, Gramolelli S, Damas M, Dittrich-Breiholz O, Kracht M, Rückert J, Varga Z, Keri G, Schulz TF. 2013. The inflammatory kinase MAP4K4 promotes reactivation of Kaposi's sarcoma herpesvirus and enhances the invasiveness of infected endothelial cells. PLoS Pathog 9:e1003737. https://doi.org/10.1371/journal.ppat.1003737.
96. Carpenter AE, Jones TR, Lamprecht MR, Clarke C, Kang IH, Friman O, Guertin DA, Chang JH, Lindquist RA, Moffat J, Golland P, Sabatini DM. 2006. CellProfiler: image analysis software for identifying and quantifying cell phenotypes. Genome Biol 7:R100. https://doi.org/10.1186/gb-2006-7-10-r100.
97. Roskoski R, Jr. 2015. Classification of small molecule protein kinase inhibitors based upon the structures of their drug-enzyme complexes. Pharmacol Res 103:26–48. https://doi.org/10.1016/j.phrs.2015.10.021.